

### “WHAT IS ALL THIS SPUTTERING NONSENSE ANYWAY?”

A few years ago, a medical conference and a sputtering conference were taking place simultaneously at Imperial College. The conferees were as always demonstrating the well-known scientific phenomenon that conference systems tend towards a condition of being in the bar, where a well-oiled medic accosted a group of the sputterers and demanded to know “What is all this sputtering nonsense, anyway?”. “Well”, replied one of the sputterers, “we’re in a branch of the medical profession too, old chap – in speech therapy actually. Sputtering’s like stuttering, you know, except our chaps say p . . . p . . . p . . . p . . . instead of t . . . t . . . t . . . t . . .”. The medic warmly thanked his newly-discovered professional colleague and hurried back to enthusiastically convey the freshly-gleaned information to his cronies.

The medic might have been a bit closer, though not very much, if he had looked in the dictionary. It seems that the word ‘sputter’ appeared in the English language (The Shorter OED, 1959) as early as 1598 and is adapted from the imitative words ‘sputteren’ in Dutch and ‘sputterje’ in West Frisian. ‘To spit out in small particles and with a characteristic explosive sound’, says the dictionary; ‘to utter hastily and with the emission of small particles of saliva, to ejaculate in confused, indistinct or uncontrolled manner, especially from anger or excitement – His tongue was too large for his mouth; he stuttered and sputtered (1878)’.

Compared with the above, you may be disappointed with the type of sputtering I’m going to describe. I must confess that I have never heard the sound of sputtering, although the sound of rotary pumps will ring in my ears forever. On the other hand, my type of sputtering is rather colourful!

### INTERACTIONS OF IONS WITH SURFACES

Let us consider what happens when an ion approaches the surface of a solid (of the same or different material); the solid is usually called the *target*. One or all of the following phenomena may occur (Figure 6-1):

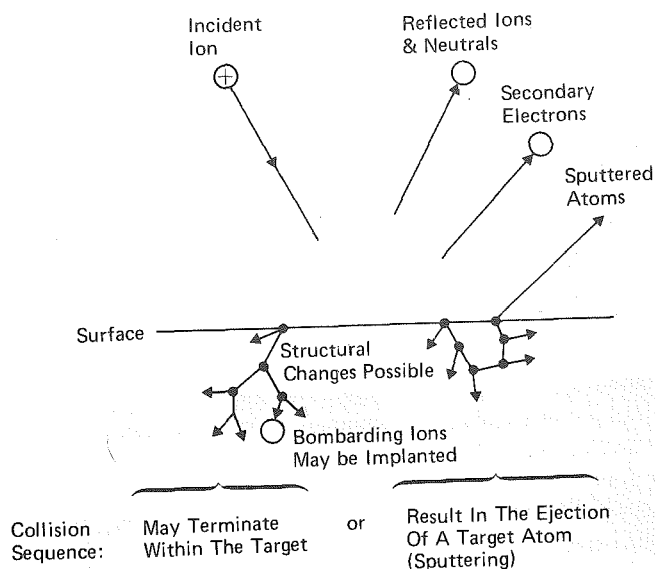


Figure 6-1. Interactions of ions with surfaces

- The ion may be reflected, probably being neutralized in the process. This reflection is the basis of an analytical technique known as *Ion Scattering Spectroscopy*, which enables us to characterize the surface layers of the material, and also tells us a lot about the fundamental ion-surface interaction.
- The impact of the ion may cause the target to eject an electron, usually referred to as a *secondary electron* (Chapter 4, "Secondary Electron Emission").
- The ion may become buried in the target. This is the phenomenon of *ion implantation*, which is already used extensively in integrated circuit technology for selectively doping silicon wafers with precisely controlled amounts and depth profiles of specific impurities, and is likely to find many other applications such as surface treatment of steels.
- The ion impact may also be responsible for some structural rearrangements in the target material. 'Rearrangements' may vary from simple vacancies (missing atoms) and interstitials (atoms out of position) to more gross lattice defects such as changes of stoichiometry (i.e. relative proportions) in alloy or compound targets, or to changes in electrical charge levels and

distributions, and are usually collectively referred to as *radiation damage*, which is a subject of great importance, particularly with relation to nuclear energy. Radiation damage can often be removed by annealing (heat treatment) but it is not always unwanted, and perhaps the alternative name of *altered surface layers*, used mostly to describe the stoichiometry changes, is more apt.

- The ion impact may set up a series of collisions between atoms of the target, possibly leading to the ejection of one of these atoms. This ejection process is known as *sputtering*.

### The Mechanisms of Sputtering

In the energy range most relevant to sputter deposition, the interaction between the impinging ion and the target atoms, and the subsequent interactions amongst the latter, can be treated as a series of binary collisions. The sputtering process is very often compared to the break in a game of atomic billiards (Figure 6-2) in which the cue ball (the bombarding ion) strikes the neatly arranged pack (the atomic array of the target), scattering balls (target atoms) in all directions, including some back towards the player, i.e. out of the target surface. In the real process, the interatomic potential function (the variation of interatomic repulsion or attraction with separation distance) is rather different from the hard sphere billiard ball case, but nevertheless the billiard model is not too unrealistic.

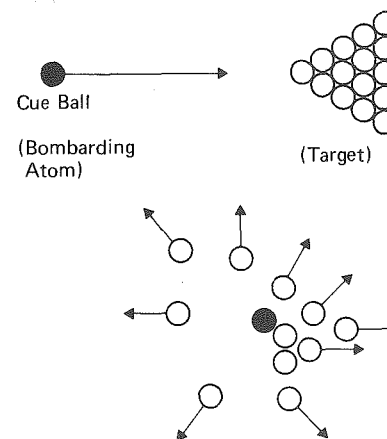


Figure 6-2. Sputtering – the atomic billiards game

It is implied in our description of the basic interaction that the incident particle could be either an ion or a neutral atom. Ions are normally used since they can easily be accelerated by an electric field, whereas neutrals pose a problem in this respect. Furthermore, the ions are likely to be neutralized anyway by the Auger emission of an electron from the target as the ion approaches, so that the impacting species are actually mostly neutral.

The series of collisions in the target, generated by the primary collision at the surface, is known as a *collision cascade* (Figure 6-1). It will largely be a matter of luck whether this cascade leads to the sputter ejection of an atom from the surface (which will require at least two collisions) or whether the cascade heads off into the interior of the target, gradually dissipating the energy of the primary impact, ultimately to lattice vibrations, i.e. heat. It's not surprising then that sputter ejection is rather inefficient, with typically 1% of the incident energy reappearing as the energy of the sputtered atoms.

The collision phenomena occurring in a target, often referred to as *target kinetics*, are a fascinating and important subject for study. They relate not only to sputter deposition and etching, but also to ion implantation and radiation damage. Life is rather short, however, and there is neither room in this book nor am I adequately informed to pursue the topic much further. But in this chapter we shall be looking at the applications of sputtering rather than the collision phenomena leading to sputtering, and fortunately we need consider only certain aspects of the process in order to do this. In the next section we shall look briefly and (unfortunately) superficially at some of the quantitative relationships involved in sputtering target kinetics.

### Sputtering Target Kinetics

A generalized treatment of target collision phenomena would have to consider the detailed interatomic potential function, but fortunately the interactions in a sputtering target are sufficiently short range that we need consider interactions only between immediate neighbours (including the incident ion). A binary collision is characterized by the energy transfer function which we met earlier (Chapter 1, "Energy Transfer in Binary Collisions"):

$$\frac{4m_i m_t}{(m_i + m_t)^2}$$

where  $m_i$  and  $m_t$  are the masses of the colliding atoms. The sputtering process is the result of a series of such collisions. A detailed consideration and experimentation show that the binary model is a useful representation of the interactions under sputtering conditions.

A useful parameter that we shall encounter frequently is the *sputtering yield*  $S$ , defined as the number of target atoms (or molecules) ejected per

incident ion. From our model above, we would expect the sputtering yield to depend on the masses of the incident ion and the target atom,  $m_i$  and  $m_t$  respectively, and on the energy  $E$  of the incident ion. However, consider sputtering as the overall process of transferring energy from the incident ion to the sputtered atoms. Then, since the sputtered atoms can come only from the surface layers of the target, it is not just a question of transferring energy to the target atoms, but also that this energy should be transferred mostly to the surface layers. We would therefore expect the sputtering yield  $S$  to be proportional to the energy deposited in a thin layer near the surface, and this is determined by the *nuclear stopping power*  $s(E)$ ; for low bombardment energies up to about 1 keV, an expression due to Sigmund (1969), which not surprisingly involves the energy transfer function, is

$$s(E) = \frac{m_i m_t}{(m_i + m_t)^2} E \times \text{constant}$$

and this is used to predict the following form for the sputtering yield  $S$ :

$$S = \frac{3\alpha}{4\pi^2} \frac{4m_i m_t}{(m_i + m_t)^2} \frac{E}{U_0}$$

Here  $U_0$  is the surface binding energy of the material being sputtered, and  $\alpha$  is a monotonic increasing function of  $m_t/m_i$  which has values of 0.17 for  $m_t/m_i = 0.1$ , increasing up to 1.4 for  $m_t/m_i = 10$ .

This expression for  $S$  predicts that the yield will increase linearly with  $E$ . In practice, this seems to be satisfied up to above 1 keV, above which  $S$  becomes relatively constant; Figure 6.3a is typical. It appears that the higher input energy is being distributed through a larger volume, so that the energy transmitted to the surface layers remains virtually constant. At very high energies,  $S$  even decreases as ion implantation becomes dominant (Figure 6-3b).

So our original expression for  $S$  is apparently valid only up to about 1 keV, and this is due to various assumptions about the atomic interactions. Above 1 keV, a modified interaction yields

$$S = 3.56\alpha \frac{Z_i Z_t}{(Z_i^{2/3} + Z_t^{2/3})} \frac{m_i}{(m_i + m_t)} \frac{s_n(E)}{U_0}$$

where  $s_n(E)$  is a reduced stopping power and is a function of a reduced energy based on the actual energy, masses and atomic numbers  $Z_i$  and  $Z_t$  of the atoms involved. The interested reader is referred to Winters (1976) for further details.

The success of these theoretical models can be demonstrated by comparing experimental and theoretical results, with good agreement resulting in most cases. This is illustrated in Figure 6-4 for the case of argon on copper, which compares the yield predicted by the equation above, with experimental values.

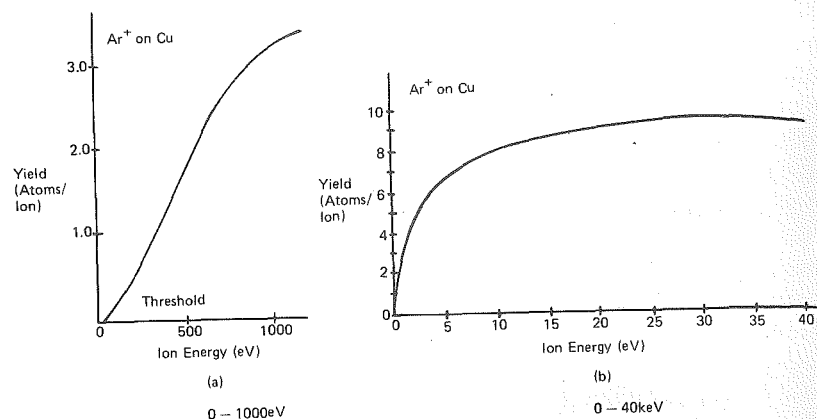


Figure 6-3. The variation of sputtering yield, for argon ions on copper, as a function of the ion bombardment energy (Carter and Colligon 1968)

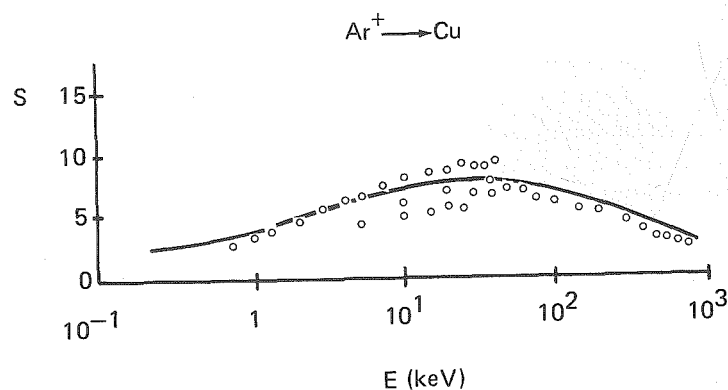


Figure 6-4. Theoretical (solid line) and experimental values for the energy dependence of the sputtering yield of copper in argon. Data from various authors; see Winters (1976)

It is apparent from examining the two sputtering yield expressions that we should no longer expect to find a maximum yield when  $m_i = m_t$  as suggested by the energy transfer function alone. This prediction seems to be borne out in practice: Figure 6-5 shows the results obtained by Almen and Bruce (1961) for the sputtering of copper by inert gas ions over a wide range of ion energies.

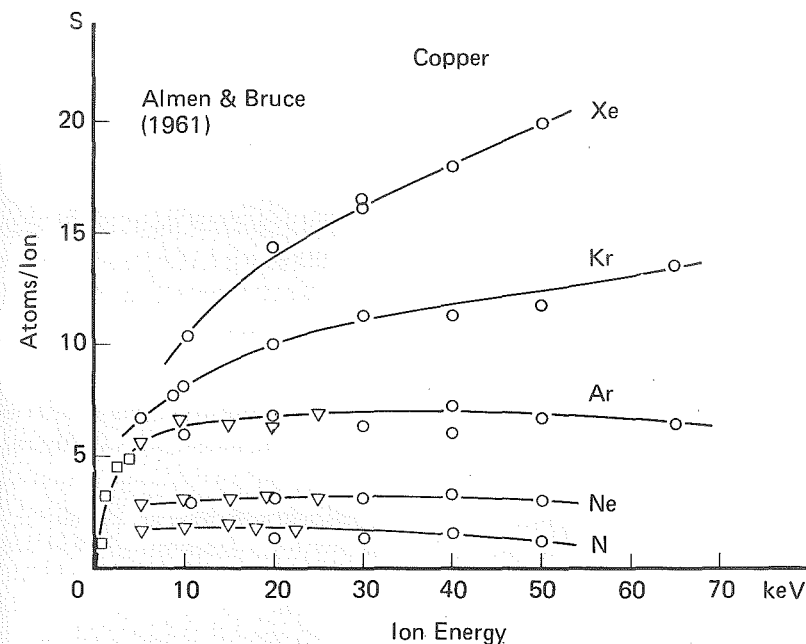


Figure 6-5. Sputtering yields of the noble gases on copper, as a function of energy (Almen and Bruce 1961)

These results show that the sputtering yield  $S$  obtained with xenon (atomic weight 131) is the largest of all these gases at all energies, even though the masses of krypton (83) and argon (40) are much closer to that of copper (64).

The high energy ( $> 1$  keV) expression for  $S$  is reasonably successful at predicting the observed mass dependences but the low energy yield expression shows quite the wrong mass dependence. And indeed, the low energy model becomes quite incorrect for energies below 100 eV, which is an energy range which we shall discuss further in connection with bias sputtering.

The sputtering model which we used above shows only the general features of the process. A more accurate model is being developed and the interested reader should refer to the review articles by Wehner and Anderson (1971), Townsend and Kelly (1976), Winters (1976), and Kelly (1978). A realistic model is rather complex: for example, one has the pragmatic consideration that a sputtering target eventually becomes a mixture of the original target and the bombarding element embedded in or otherwise combined with it, so that one is no longer dealing with the sputtering of the original target. Never-

theless, we shall see that the simple ideas discussed above will be quite valuable when we consider later how the sputtering process is put into practice.

In the appendix to this chapter, we have shown more sputtering yield data, concentrating on typical sputtering ion energies and the usual sputtering gas, argon.

### Summary of the Overall Process

Although we have looked a little at what's going on in the target, that knowledge isn't really essential to an understanding of sputter deposition. What we do need to know, however, is what the overall results of these target processes are (Figure 6-6):

- A target atom may be sputter ejected.
- The incident ion will either become implanted or be reflected, probably as a neutral and probably with a large loss of energy.
- The ion impact and the resulting collision cascade will cause an amount of structural reordering in the surface layers.
- A secondary electron may be ejected.

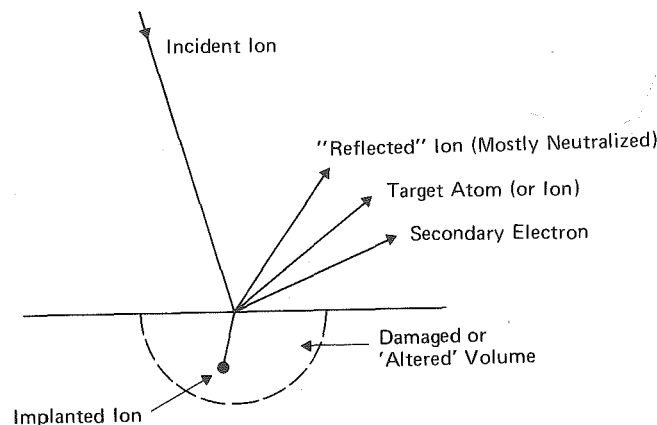


Figure 6-6. Summary of the target processes

These are just *possible* consequences of the impact; the possibilities will not generally occur in any specific ratio, nor even necessarily occur at all. We shall see shortly how each of these aspects of the sputtering process are manifested and/or utilized.

## APPLICATIONS OF SPUTTERING

### Sputter Etching

As we have already seen, the sputtering process essentially involves knocking an atom out of the surface of a target. By repeating this process over and over again, we can evidently *sputter etch* the target. We may wish to do this over the whole of the target surface, for example to clean it or to make it thinner, or selectively to generate a topographic pattern on the surface. We shall return to this application later in the chapter.

### Sputter Deposition

The ejected atom can also be used. After ejection it can, under the right circumstances, move through space until it strikes and condenses on the surface of a receiver, which is known as a *substrate*. By repeating the process over and over, we can build up a coating of several or many atomic or molecular layers of target material on the substrate. The coating, which is generally less than about 1  $\mu\text{m}$ , is called a *thin film*, and the process is known as *sputter deposition*; this process is currently the main application of sputtering.

Although I shall be frequently referring to the properties of thin films prepared by sputter deposition, there is no room here for a general treatment of thin film science, although the initial formation and growth stages are discussed below (in "Thin Film Formation"). The reader who has no background in this area is advised to read one of the several reviews on the subject (Berry, Hall and Harris 1968, Lewis and Campbell 1967, Chapman and Jordan 1968, Neugebauer 1970, Leaver and Chapman 1971; the last is very elementary).

### Limitations of Sputtering

There are some devotees of sputtering who would claim that anything can be sputtered. There are others who would claim that if a material can't be sputtered then that material isn't worth bothering with!

These views are rather extreme, though it's certainly true that sputtering is a widely applicable and versatile process. How then do we decide whether to sputter? When it comes to specific applications and specific materials, there are so many factors to be considered that it would be misleading of me to generalize. However, ignoring my own advice, there are a few general restrictions. The capital expenditure for sputtering equipment is higher than for virtually all other coating processes. As a coating or etching process, it's too slow for some applications (for a review of the many other surface coating techniques available, see Chapman and Anderson 1974). Deposition rates are

typically 50 — 500Å per minute, and etch rates around 500 — 10,000Å per minute, although there are higher rate versions of the process available.

As we shall see, sputtering is carried out in partial vacuum and there are some materials which are incompatible with good vacuum practice, either due to their inherent properties or due to their products under the various types of bombardment involved in the process. Organic solids are frequently unable to withstand this bombardment, and completely degrade; the temperature rise alone is often adequate to produce this effect. On the other hand, it is remarkable that polytetrafluoroethylene, which has a long chain molecule and cannot possibly be sputtered intact, and which can easily be reduced to a carbonaceous mess at quite low temperatures, can nevertheless be sputtered to produce quite useful films with properties similar to those of the target.

The presence of the vacuum pumps also means that one frequently encounters problems when using target materials containing volatile components. The resulting films are often deficient in the volatile component, although this can sometimes be rectified.

To summarize, sputtering is a rather versatile process. It's applicable widely but naturally has some shortcomings and drawbacks. One is advised to read the published literature on specific applications and specific materials before becoming too enthusiastic.

We now begin to look at some of the details of the process by considering a dc sputtering system. Actually, most sputtering systems are rf driven, but it is helpful to first look at the dc counterpart.

### A CONVENTIONAL DC SPUTTERING SYSTEM

In this section we shall meet briefly some ideas which are discussed in more detail later. This probably means that this will make more sense after you've read later sections. On the other hand, I think you should read this first so that you see the overall picture before we plunge into the detail.

How do we deposit thin films by sputtering? It's very informative to look at a conventional dc sputtering system (Figure 6-7) to see the elements used to turn the sputtering phenomenon discussed in the last section into a practical deposition process.

The material we wish to sputter is made into a *sputtering target* which becomes the cathode of an electrical circuit, and has a high negative voltage  $V$  (dc) applied to it. The target is nearly always solid, although powders and even liquids are sometimes used. The substrate which we wish to coat is placed on an electrically grounded anode a few inches away. These electrodes are housed in a chamber which is evacuated. Argon gas is introduced into the chamber to some specified pressure. The action of the electric field is to accelerate electrons

### A CONVENTIONAL DC SPUTTERING SYSTEM

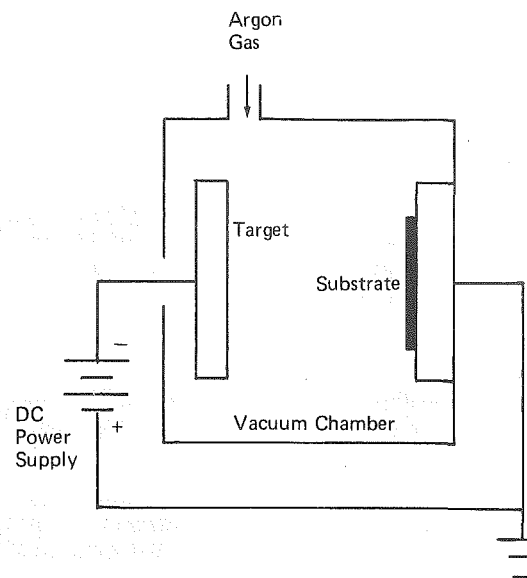


Figure 6-7. Schematic of a dc sputtering system

which in turn collide with argon atoms, breaking some of them up into argon ions and more electrons to produce the glow discharge that we discussed in Chapter 4. The charged particles thus produced are accelerated by the field, the electrons tending towards the anode (causing more ionization on the way) and the ions towards the cathode, so that a current  $I$  flows.

When the ions strike the cathode, they may sputter some of the target atoms off. They may also liberate secondary electrons from the target and it is these secondary electrons which are responsible for maintaining the electron supply and sustaining the glow discharge (Chapter 4, "Maintenance of the Discharge"). The sputtered atoms from the target fly off in random directions, and some of them land on the substrate (on the anode), condense there, and form a thin film.

The voltage  $V$  which is required to drive the current  $I$  through the system is a function of the system pressure  $p$ . The rate of thin film formation on the substrate will depend on the amount of sputtering at the target; this in turn will depend on the ion flux at the target and so (linearly) on the current. However, the amount of sputtering also depends on the sputtering yield  $S$  and so on the ion energy and hence on  $V$ , which determines the sheath voltage at

the target. The choice of sputtering pressure  $p$  and the implied choice of the V-I characteristic, are thus rather important and so we'll now look at the criteria used in selecting operating parameters and in deciding on the nature of the sputtering gas.

### Choosing the Sputtering Gas

As we saw earlier, it doesn't really matter whether we use neutral atoms or ions as far as the actual sputtering process is concerned. However, it is easy to accelerate ions to the energies required by using an electric field and much more difficult to accelerate neutrals; so we normally use ions.

It's much easier to ionize atoms when they are in a gaseous state, and naturally the latter state is easier to achieve with materials already in a gaseous form at room temperature. So we use gases for our ion source. A glow discharge happens to be a particularly convenient method of producing a significant flux of gas ions.

We usually don't want the ions to react with the target or growing film, which therefore requires noble gas ions. We shall see later that some sputtering ions will become incorporated into the growing film and become trapped by the depositing film atoms. Since we are usually concerned with the purity of the film, we'd prefer these incorporated ions to be as innocuous as possible; this is another reason for using noble gas ions, with their closed shell electronic structures and (almost always) chemical inactivity. We saw earlier that the heaviest inert gas will give the highest sputtering yield (Figure 6-5). Radon ( $Z=86$ ) is the heaviest, but it is also radioactive. Xenon (54) and krypton (36) are next in line, but argon (18) is almost always used in sputter deposition because it is easily available and cheaper, and the sputtering yield is only a factor of about two down on xenon at sputter deposition energies. The cost of the sputtering gas is not usually a significant factor, though, because a cylinder may last a year in a small sputtering system. Most gas suppliers have several grades of argon; their standard grade is usually intended for applications such as argon arc welding, and is not pure enough for sputtering.

### Choosing the Pressure Range

A vacuum system enables us to control the operating pressure inside the sputtering system. Operating pressure limitations are imposed by the requirements of both the glow discharge and of film deposition.

The glow discharge sets a lower pressure limit. The discharge is sustained by electrons making ionizing collisions in the gas. The number of ionizing collisions will decrease with decreasing gas density, and hence gas pressure, so that the discharge current (for constant voltage) will also decrease. This is shown for

a typical case in Figure 6-8. Below about 30 mtorr, the current (and hence ion flux at the target) and sputtering rate in a dc discharge become quite small.

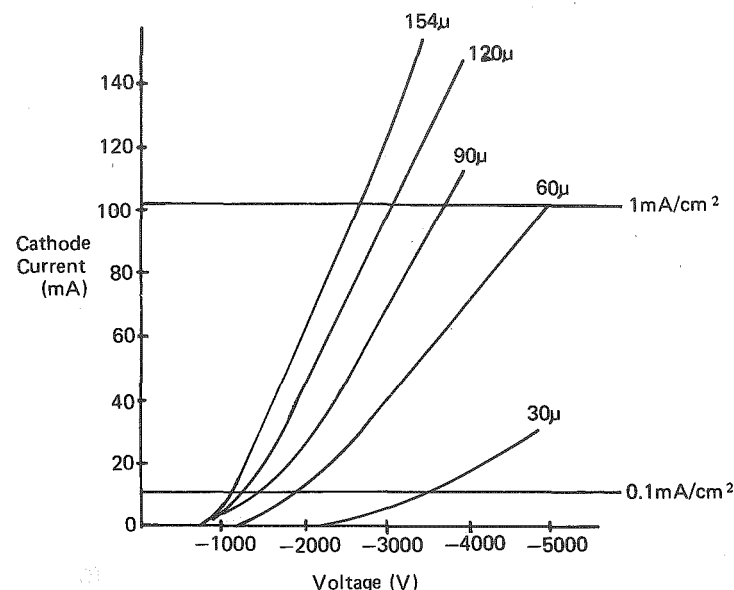


Figure 6-8. Typical I-V curves at different argon pressures using a 4½ inch nickel cathode - area 103 cm² (Kay 1969)

A different problem arises at the other end of the pressure range. In the same way that electrons undergo collision, material sputtered from the target may collide with gas atoms on its way to the substrate, at a rate which will increase with increasing pressure; we discussed this in Chapter 1, "Probability of Collision". The result of the collision is to deflect the sputtered atom, sometimes back towards its parent, and hence decrease the deposition rate. This is demonstrated in Figure 6-9, which shows how the apparent sputtering yield of a nickel target (obtained by measuring its weight loss) decreases with increasing pressure due to sputtered nickel being backscattered in the gas phase and redeposited on the target. The mean free path (see Chapter 1) of the nickel is about 1 mm at 120 mtorr, so this result is expected. With increasing pressure, deposition becomes less a line-of-sight process and more a diffusion process. The scattering process becomes serious above about 100 mtorr, so that taking both of our limi-



tations into account, an overall operating range of about 30 – 120 mtorr is usual for dc sputter deposition. This isn't a very wide operating range, but at least the two limits haven't overlapped! Later we'll see modifications of the basic sputtering process which permit lower operating pressures.

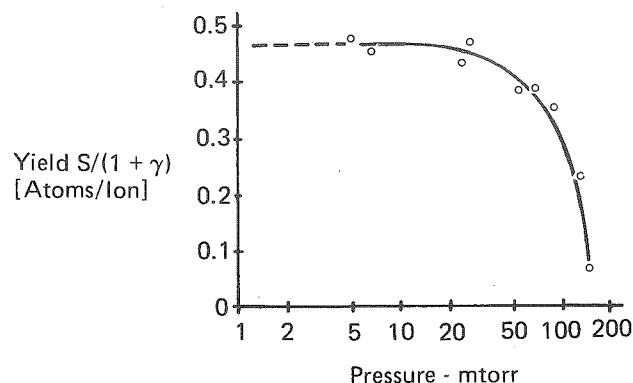


Figure 6-9. Variation of the apparent sputtering yield of nickel vs argon gas pressure; 150 eV ion energy (Laegreid and Wehner 1961)

### Choosing Electrical Conditions for the Glow Discharge

We have an operating range of 30 – 120 millitorr, but what voltage and current should we use? To some extent that is Hobson's choice since, for each operating pressure, target material and sputtering gas, there is a specific voltage – current relationship. The V-I relationships at several pressures, for a nickel target sputtered in argon, are shown in Figure 6-8. Actually the target material isn't that important even though the secondary electron coefficient  $\gamma$  does vary from material to material. Table 6-1 shows the current densities obtained from various target materials under similar conditions, and the densities are very much alike, at least for this restricted case of conducting targets.

The sputtering rate of the target is determined by the flux of ions and energetic neutrals, and the sputtering yield. An ion current of 1 mA/cm<sup>2</sup> corresponds to a flux of  $6 \cdot 10^{15}$  singly charged ions per cm<sup>2</sup> per second. However, the target current also includes a secondary electron component, and the target bombardment flux is due to energetic neutrals as well as ions.

Figure 6-8 suggests that, by applying a high enough voltage, we could have any target current we want. But maybe that's the wrong approach. What ion

Table 6-1

Target current density as a function of target material and discharge gas. This data was acquired over a period of years and is presented to show that the target current density is relatively insensitive to target material and additive gases. Target voltage = -2000 V, gas pressure 70 mtorr, and interelectrode spacing ~4 cm. From Winters et al. (1977)

Target Material	Current Density (mA/cm <sup>2</sup> )	Gas
Si	1.35	CF <sub>4</sub>
Si	1.25	CF <sub>4</sub> + 6½% O <sub>2</sub>
Si	1.20	CF <sub>4</sub> + 10½% O <sub>2</sub>
Si	1.05	CF <sub>4</sub> + 16% O <sub>2</sub>
Si	1.15	CF <sub>4</sub> + 22½% O <sub>2</sub>
Si	1.30	CF <sub>4</sub> + 34% O <sub>2</sub>
Si	1.35	CF <sub>4</sub> + 42% O <sub>2</sub>
Si	0.45	Ar
Mn <sub>5</sub> Ge <sub>3</sub>	0.55	Ar
GdFe	0.69	Ar
CoNi	0.49	Ar
Ni	0.46	Ar
CoNi	0.42	Ar
Ti	0.43	Ar
V	0.43	Ar
Ag	0.49	Ar
C	0.41	Ar
Ta	0.63	Ar
Ni	0.56	Ar + 10% N <sub>2</sub>
Au	0.39	Ar + 10% N <sub>2</sub>
Au	0.51	Ar + 10% N <sub>2</sub>
W	0.51	Ar + 10% N <sub>2</sub>
W	0.49	N <sub>2</sub>
Ni	0.44	N <sub>2</sub>



energies should we use for sputtering? We saw earlier that the sputtering yield rises monotonically with ion energy up to several tens of keV, where it begins to decrease. This latter region, where we're getting less for more, is obviously not an energy bargain basement but what other criteria are important? A prime matter is that of safety. Electrically we'd like low voltages and because X-rays can be produced by fast ions and electrons, we ought to keep energies and voltages below 10 kV. Within this limit, many other criteria become important and so the material being deposited and the requirements made of it must be considered. The broad range, though, is usually determined by the fact that we will be restricted (if only economically) to a sputtering power supply of limited output. By varying the operating pressure of the sputtering system, we can change the V-I relationship of the discharge (within certain limits) whilst maintaining the same power input VI. So rather than consider only the sputtering yield  $S$ , we need to look also at the yield per energy input,  $S/E$ ; this is shown in Figure 6-10 for the case of xenon on copper, and in Figure 6-11 for argon on tungsten over a narrower energy range. These suggest a most efficient ion energy of a few hundred volts. Other materials would give similar results.

This dependence of  $S/E$  on  $E$  is not too surprising. Our sputtering kinetics model ("Sputtering Target Kinetics") suggested that  $S$  should increase linearly with  $E$  up to about 1 keV. If so, then  $S/E$  should be constant, and this seems to be the case except below about 100 eV, where the model begins to break down. Above 1 keV or so, the sputtering yield is fairly constant, so that  $S/E$  falls with increasing energy.

Several points, which are discussed in Chapter 4, have to be stressed. A V-I discharge relationship does not mean that the flux of sputtering particles at the cathode is equivalent to  $I$ , since some of the cathode current is carried by electrons, and some of the sputtering particles are neutral. It also doesn't mean that the sputtering particles will all have an energy of  $V$  electron volts; instead they will have a wide energy distribution with a maximum of  $V$  because they too (like the electrons) collide with gas atoms and usually slow down in the process.

Another way of saying all of the above is that not all of the VI power input goes into the target. Of course there is no general reason why we should try to get the maximum amount of sputtering per unit energy input, since there may be other more important criteria governing our choice of V-I such as a particular operating pressure or a low operating voltage.

The sputtering yield per unit energy input ( $S/E$ ) data tell us that we shouldn't expect to sputter very rapidly below about 100 V and that the process is becoming very inefficient above 10 kV. In practice, a lower limit of about 500 V is used to achieve adequate current density, and an upper limit above 5 kV is rarely found necessary. Even with a sheath voltage of 500 V, the ion bombardment

energy is generally much lower because of charge exchange collisions in the sheath.

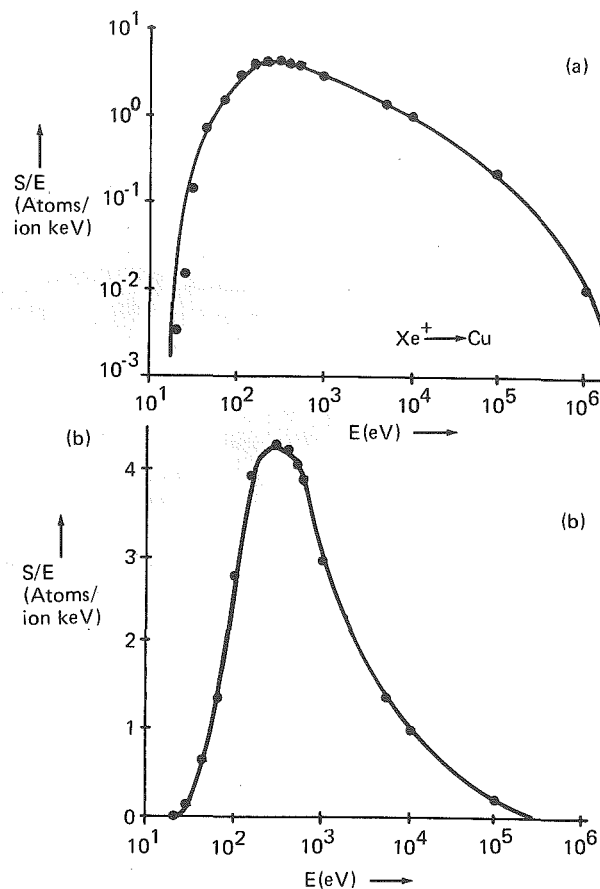


Figure 6-10. Variation of the sputtering yield per unit energy input of xenon on copper vs ion energy. Data from: Dupps and Scharman (1966), Almen and Bruce (1961), Guseva (1960), Wehner (1962), Stuart and Wehner (1962)

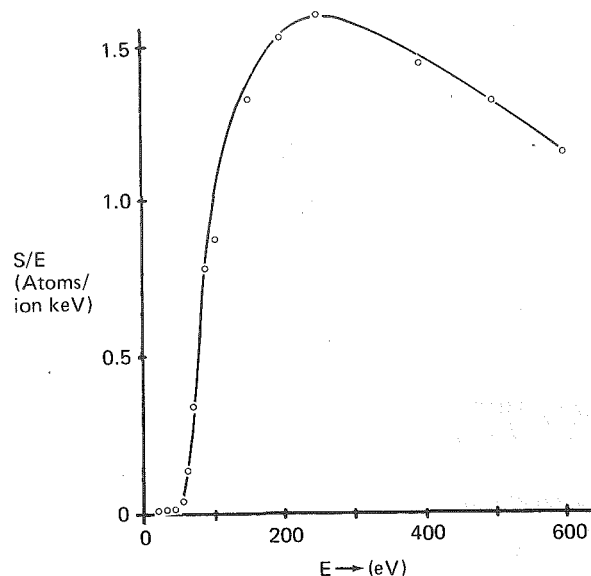


Figure 6-11. Variation of the sputtering yield per unit energy input for argon on tungsten vs ion energy. Data from: Stuart and Wehner (1962), Wehner (1962)

### Summary

We have seen in outline how sputter deposition can be carried out in a dc system using a glow discharge as an ion source. The ions are usually of a noble gas which is introduced into the system and maintained at a pressure in the 30-120 millitorr range. The voltage required to maintain a glow discharge having a current density of 0.1 - 2.0 mA/cm<sup>2</sup> is usually in the range 500 - 5000V.

In the next sections we shall look more closely at sputtering discharges so that we can better understand and control the sputter deposition process.

### SPUTTER ETCHING AND DEPOSITION OF INSULATORS

In the previous discussion of a dc sputtering system, it was assumed that the target was conducting, or at least reasonably so. One wouldn't want to drop more than about 100 V across the target, so with typical numbers of 1 mA/cm<sup>2</sup> for the target current density and 0.5 cm for the target thickness, this sets a limit of  $\rho = 2 \times 10^5 \Omega\text{cm}$ , which is quite resistive. So some nominal insulators could be sputtered, but it isn't usually a very good solution because of problems such as stress developed in the target by the resistive heating there.

Instead, two common ways of depositing insulating thin films are by *rf sputtering* and *reactive sputtering*.

### RF Sputtering

The technique of rf sputtering uses an alternating voltage power supply at rf frequencies around 10 MHz, so that the sputtering target is alternately bombarded by ions and then electrons so as to avoid charge build-up. The rf discharge was discussed in some detail in Chapter 5, where we also looked at the choice of operating frequency, crystal controlled and self-excited oscillators, and matching networks. It also seemed that the rf discharge made more efficient use of the electron impact ionization, so that operating pressures could be practically extended down to 1 mtorr. Because the detail of the sheath mechanism is slightly different in the rf case, the sheath is still about 1 cm thick at 10 mtorr, and so the lower pressure leads to less ion energy attenuation due to charge exchange. The lower operating pressure also reduces the amount of scattering of material sputtered from the target (cf. Figure 6-9).

There are more subtle advantages: in dc sputtering systems, *arcing* is sometimes a problem, due to patches of dirt (with higher secondary electron coefficient), pockets of outgassing (higher pressure, higher  $j$  locally), or asperities (higher  $E$ ). These *unipolar arcs* (Maskrey and Dugdale 1966) can be quite troublesome, leading to the necessity of *conditioning* a sputtering target before general usage, by slowly increasing the applied power and sputtering (or evaporating) away the arc-forming defect.

These arcs are less likely to form in rf discharges because the field is maintained in one direction for less than one cycle, and reduces to zero twice in each cycle, making it more difficult for the arc to be sustained. Even so, target conditioning is still necessary.

With its various advantages, rf discharges are almost always used for sputtering purposes. The two principal exceptions are magnetron sputtering systems and ion beam sputtering systems; these are discussed later.

### Reactive Sputtering

Reactive sputtering avoids the problem of target charging instead of solving it. A conducting elemental target is dc sputtered, and the sputtered material is combined chemically with a component from the gas phase, e.g. oxygen. In Chapter 7, we shall see how electron impact dissociation can turn the discharge into a chemically active environment. To illustrate the technique, silicon nitride can be produced by sputtering silicon in a dc (or rf) discharge containing nitrogen. Even when a compound target is rf sputtered, reactive sputtering is often

used to restore the stoichiometry of the film. We shall return to this topic in "Deposition of Multicomponent Materials".

### PRACTICAL ASPECTS OF SPUTTERING SYSTEMS

In the previous section, we dealt with some of the process conditions required for sputtering. Of course, there are many other practical considerations in making a sputtering system. This book is primarily about the glow discharge aspects of the process, and so such details are discussed only briefly.

#### Ground Shields

Looking into a sputtering system, one is immediately aware of several features (Figure 6-12). The target is surrounded by a *dark space shield*, also known as a *ground shield*. The purpose of this is to restrict ion bombardment and sputtering

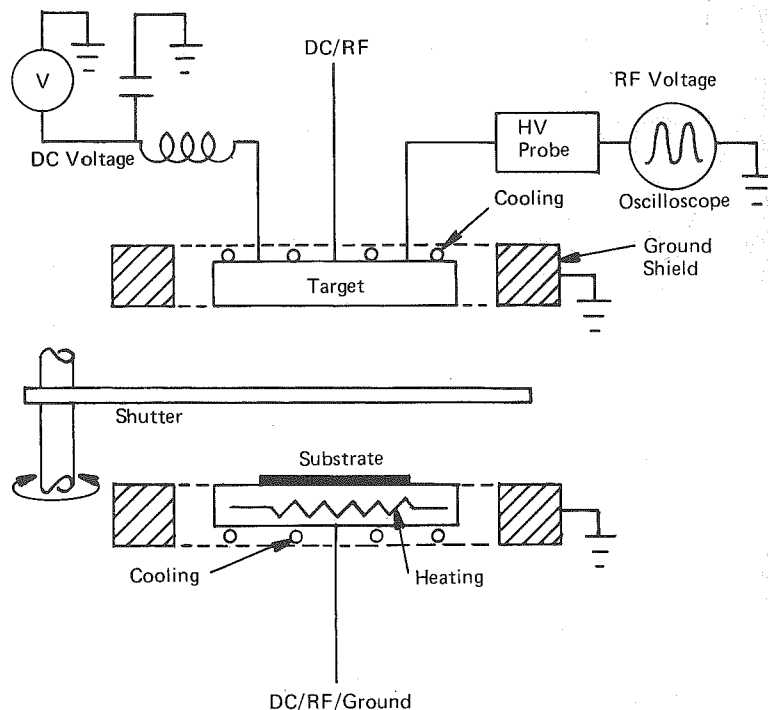


Figure 6-12. Schematic of a sputtering system showing ground shields, shutter, electrode cooling and heating, rf and dc voltage measurement

to the target only. Otherwise, the target backing plate, mounting clips (if any) and mechanical supports would also be sputtered and cause the film to be contaminated. In order to prevent ion bombardment of the protected regions, the space between the target and the ground shield must be less than the thickness of the dark space. From the descriptions of the glow discharge maintenance mechanisms in Chapters 4 and 5, we can see that this criterion is such as to prevent the establishment of a self-sustained discharge in the space between the target and the shield. Occasionally one finds that sharp points or patches of dirt cause local discharges or arcs, particularly with dc discharges, and these must be eliminated. Some possible ground shield arrangements are shown in Figure 6-13.

Since the thickness of the dark space decreases with pressure, the size of the gap between the target and shield sets an upper pressure limit for operating the system. In principle, the gap could be extremely small, but in practice this is limited by spurious discharges, and in the case of rf discharges, by increasing capacitive target-to-ground coupling as the gap is decreased. The dark space thickness also decreases with frequency, so systems operating above 13.56 MHz need to have correspondingly closer ground shields.

Many systems have the capability of applying electrical power to the substrate for the technique known as *bias sputtering* (q.v.). In this case, a ground shield is required around that electrode too.

#### Shutters

Figure 6-12 shows a shutter that can be rotated into place between the electrodes. This has its use during a *presputtering* period when the first few atomic layers of the target are removed by sputtering in order to clean it. During the time that the system is open to air to load or unload it, the target is liable to become contaminated by atmospheric pollution, by handling, or by chemical combination with the atmosphere to form an oxide or other compound. If this were left in place, the first period of sputtering would transfer the contamination to the substrate. This is avoided by interposing the shutter during that initial period, in order to prevent deposition on the substrate. For the same reasons, it is often extremely helpful to clean the substrate in the same way, and to do this immediately prior to deposition so that the surface does not become contaminated. So the ability to power the substrate is useful for this pre-sputter period as well as for applying bias during sputter deposition.

One has to be careful in the use of shutters. The operating pressure range of sputtering is such that the sputtered material makes many collisions in the gas phase, and so it can diffuse around shutters to an extent. This is in contrast to the use of shutters in high vacuum ( $< 10^{-5}$  torr) evaporation where shutters block everything in the line of sight of the source.

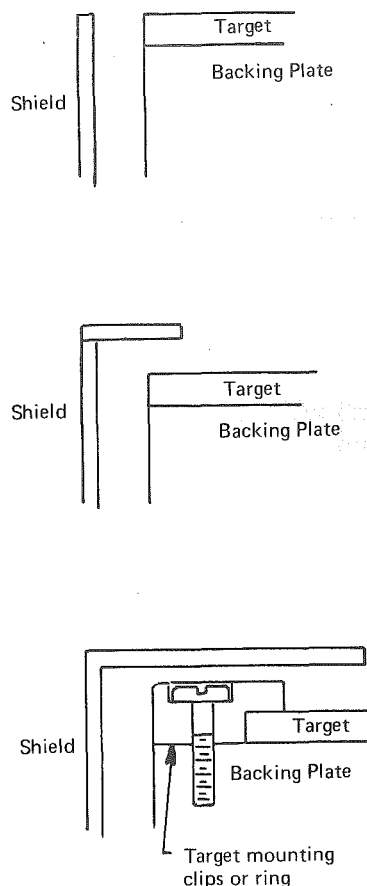


Figure 6-13. Some possible ground shield arrangements

### Target Cooling

Returning to Figure 6-12 again, we see that the target is cooled. Sputtering is a very inefficient process, and most of the power input to the system appears finally as target heating. Such heating can become excessive — local temperatures of 400° C have been reported — and can lead to damage of the bonding between the target and the backing electrode, of the target itself, of associated

vacuum O-rings, etc. This is usually avoided by cooling the target with water or another suitable liquid. On the other hand, such cooling is a complexity and it can be avoided if the power input to the target is not too great. We have successfully run several systems without cooling; indeed, this probably contributed to their reliability. There are many of us who have suffered from water leaks and their consequences! Cooling systems seem to have a propensity for blocking up and then failing at their weakest point, usually a connection. As usual, nature likes to show her influence; aluminium seems to be attacked by recirculating water systems and algae seem to thrive in rf environments, both being causes of blockage. As a last resort against water leaks, Widmer (1978) has proposed a rather 'sweet' solution, using an electromechanical arrangement with a sugar 'fuse'!

### Substrate Temperature Control

The temperature of the substrate surface is an important and yet difficult parameter to control. We shall see in the section on "Thin Film Formation" that the substrate temperature influences the formation stages of a thin film and its final structure, and in "Bias Techniques" how the temperature influences gas incorporation in the film. It is not terribly difficult to incorporate water cooling or even liquid nitrogen cooling into the substrate platform, although if the substrate platform is biased, one has to ensure that the liquid flow and its associated pipework do not cause a partial electrical short of the target by excessive resistive or capacitive coupling to ground.

Heating of the substrate platform can be achieved by circulating a hot liquid or by electrical resistance heating. If electrical isolation is required, the resistance heater can be decoupled with a suitable isolation transformer. The temperature is usually measured and controlled with a thermocouple feeding a power controller, and in this case the electrical isolation problem is a little more difficult since we need to preserve the thermoelectric emf of the couple whilst removing both the rf and dc offset components. The former may be removed by rf chokes; the latter is normally removed by using a thin insulator of mica or ceramic between the couple junction and the substrate platform or dummy substrate. In a dc sputter etch system, we have been able to successfully run the whole assembly of heater, thermocouple, and temperature controller at the dc target voltage by using a single isolation transformer at the power source, and this arrangement eliminated the need for electrical isolation (and consequent thermal isolation) between the thermocouple and substrate (Chapman et al. 1973).

There is an inherent problem in substrate temperature control in thin film deposition, whether by sputtering or evaporation. What we are really interested in is the temperature of the *surface* of the substrate rather than of its bulk, and it is difficult to measure even the latter, because of the thermal barriers inevita-

bly present, e.g. due to electrical isolation between the substrate and a thermocouple pressed down onto it, or due to thermal isolation between a substrate and the substrate platform. In this latter case, the problem arises because the substrate will generally make only three point contact to the substrate holder; it is sometimes possible to fill the intervening space with a suitable heat-conducting liquid or solid such as gallium, in order to heat-sink the substrate to the holder, but this is usually inconvenient and would be unacceptable in manufacturing processes.

The problem is exacerbated by the power input to the substrate from the glow discharge, which is liable to make the surface temperature greater than that of its bulk. The use of a thin film thermocouple evaporated onto the surface of the substrate has been proposed as a solution to this difficulty, but this is not very convenient. An alternative is to use an infra red thermometer that measures the infra red radiation emitted by the substrate; one needs to know the transmission characteristics of the window through which observation is made, but often this can be done empirically.

So it seems that measurement of the absolute substrate surface temperature is quite a difficult matter, although practically it is possible to reproduce the same conditions from run to run.

#### Electrode Voltage Measurement

Although many rf systems are controlled by the power input to the matching network and process chamber, some people prefer to measure and control with the target voltage since this eliminates the uncertain power losses in the matching network. It is more usual to measure the dc offset voltage, although the rf peak-to-peak is sometimes used. The dc voltage is normally obtained by filtering out the rf components with an LC circuit, as in Figure 6-12. The rf voltage waveform can be observed by using a high voltage probe (which is essentially a resistive network voltage divider) to reduce the rf signal to a suitable size for display on an oscilloscope. The probe is essentially a resistive or capacitive network voltage divider; if the ac and dc components of the waveform are required, the resistive type should be used. If only the rf peak-to-peak magnitude is required, a clamping circuit can be used, preferably immediately after the probe to avoid long leads carrying rf.

John Vossen has pointed out that when insulating targets are used, the dc offset voltage depends on leakage around the target edge to the backing plate; the unreliability of this can be avoided by using the peak-to-peak voltage. It is not clear to me why this leakage does not change the sputtering rate, if it really does change the target surface potential.

Whatever parameter is measured, care is required, both in safety and in interpretation. There are large rf currents flowing in the external circuitry, and the

inductance of even a straight piece of wire can become significant at radio frequencies. These combine to cause significant drops along current-carrying connecting cables, particularly that between the matching network and the target. One can observe these voltage changes with the probe . . . carefully. To obviate this problem, the probe should be attached to the back of the electrode.

All of the same considerations apply to the measurement of substrate voltage, which is almost always done in a bias sputtering system by measuring the dc offset of the applied rf.

At both electrodes, the sheath voltage is determined by the difference between plasma potential and electrode potential, as discussed in previous chapters. Christensen and Brunot (1973) have proposed a method of monitoring the sheath voltage continuously (their technique is discussed in Chapter 5) but this method has not been generally adopted. Target voltage is instead used to *reproduce* conditions rather than give absolute magnitudes.

#### SPUTTERING AS A DEPOSITION PROCESS

The current main application of sputtering is for the deposition of thin films.

##### Thin Film Formation

In sputter deposition, as with the other standard vacuum deposition process of evaporation, material arrives at the substrate mostly in an atomic or molecular form (Figure 6-14). The atom diffuses around the substrate with a motion determined by its binding energy to the substrate and is influenced by the nature as well as the temperature of the substrate. Energetically, the surface of the substrate is like an egg carton, with each of the depressions constituting a temporary resting point or *adsorption site* for the depositing and diffusing atoms. At each 'hop', the atom will either jump over the barrier into an adjacent site, or might even hop right out of the egg carton — i.e. re-evaporate. After a certain time, the atom will either evaporate from the surface or will join with another diffusing single atom to form a doublet, which is less mobile but more stable than the single atom. I like to think of two men (please insert your favourite ethnic group) tied together inside a giant egg carton, and trying to jump over the barriers into the adjacent depressions. The chance of them being well enough co-ordinated to jump together is extremely slim, so their mobility is severely limited, as is the chance of their 're-evaporation'.

The chance of forming the atomic pair will depend on the single atom density and hence on the arrival or deposition rate. In time, the doublets will be joined by other single atoms to form triplets, quadruplets and so on. This is the *nucleation* stage of thin film growth, leading to the formation of quasi-stable *islands*,

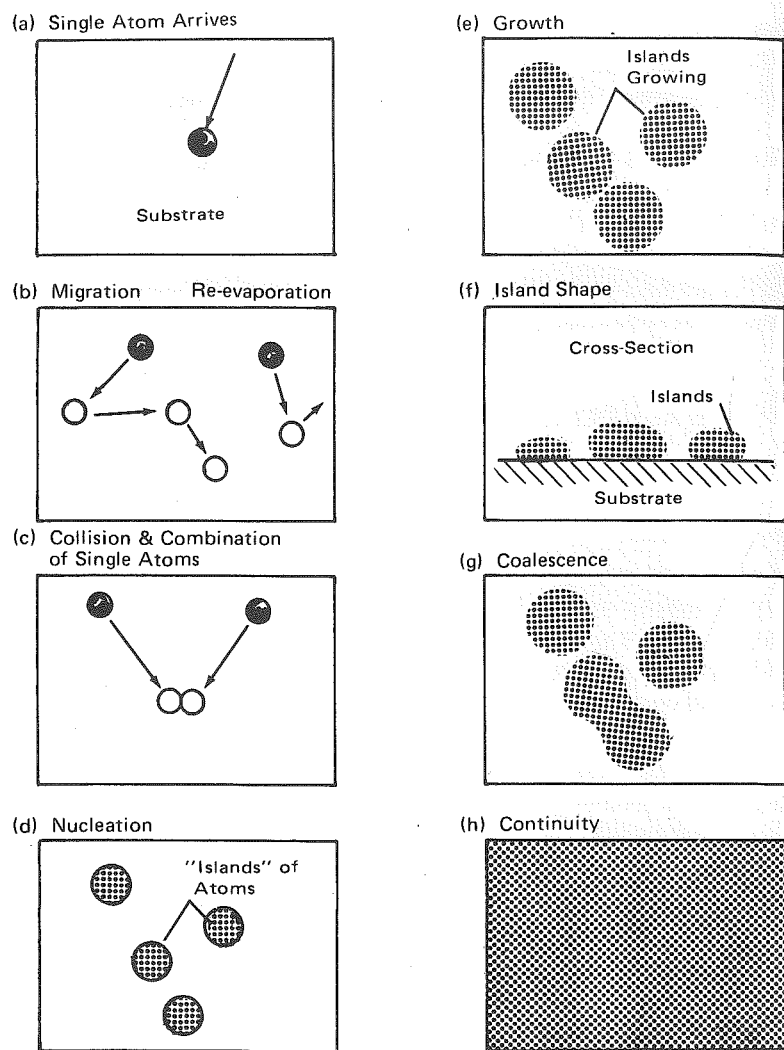


Figure 6-14. Formation of a thin film (Leaver and Chapman 1970)

each containing tens or hundreds of atoms and typically having densities of  $10^{10}/\text{cm}^2$ . During the next, *island growth* stage, the islands grow in size rather than in number. Eventually they grow large enough to touch; this is the *agglomeration* or *coalescence* stage. From observations in the transmission electron microscope, it appears that the islands often display liquid-like behaviour during coalescence, and there are often crystallographic reorientations as a result of competition between the structures of the coalescing islands. Coalescence proceeds until the film reaches *continuity*, but this may not occur in some cases until the film is several hundred Ångströms in average thickness. During the coalescence stages, the film therefore typically consists of hills and valleys.

During the island stage, each island is usually single crystal or contains just a few crystals. On a polycrystalline substrate, the orientation of each island will be random, so that the resulting film is polycrystalline. On a single crystal substrate, the island orientations may be determined by the substrate structure so that growth and coalescence leads to a single crystal film. This is the phenomenon of *epitaxy* (Bauer and Poppa 1972).

If surface atoms are mobile, they have a greater opportunity of finding low energy positions, consistent with crystal growth, in the growing film. Mobility is enhanced by increased substrate temperature. But since it also takes time to find an energetically favourable lattice position, crystal growth is also encouraged by low deposition rates. Hence, on single crystal substrates, for each deposition rate there will be a temperature, the *epitaxial temperature*, above which single crystal films can be grown.

It is more likely that polycrystalline films on polycrystalline substrates will be required. During the island stage, each island will contain one or a few crystallites. The same mechanisms obtain as in single crystal growth, so that high substrate temperature and low deposition rate lead to large grains, low density of crystal defects, and large film thickness for continuity. The reverse (low temperature and high rate) associations are also generally true.

All of the relationships above were found for the comparatively simple case of deposition by vacuum evaporation. The structure of the growing film was found to be extremely sensitive to deposition conditions. Electron bombardment either prior to or during deposition was found to encourage film continuity and reduce epitaxial temperatures (Stirland 1966). Ion bombardment (Wehner 1962) and increased arrival energy of the depositing atoms (Chapman and Campbell 1969) also reduced the epitaxial temperature.

#### Life on the Substrate

The purpose of the preceding discussion was to illustrate the very sensitive dependence of thin film structure on growth conditions, even for deposition by

evaporation. By contrast, the sputtering environment is extremely complex and has many variables.

Figure 6-15 shows a substrate on which we wish to deposit a sputtered film. We have seen that the nature and temperature of the substrate are important in determining the nature of the film. During thin film growth, the substrate and growing film will be subjected to many types of bombardment (Figure 6-16) which will now be described.

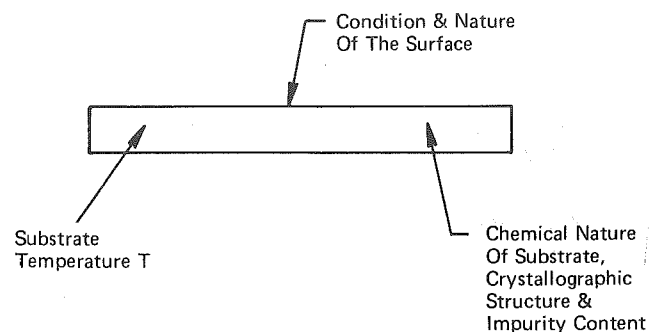


Figure 6-15. The influence of the substrate on thin film structure

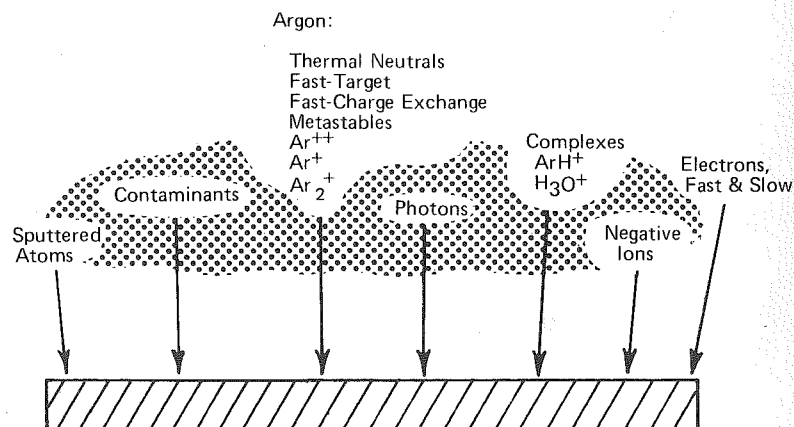


Figure 6-16. Particles bombarding the substrate in sputter deposition

### Sputtered Atoms and Contaminants

Let's refer again to the example given in Chapter 1, "Monolayer Formation Time". A typical sputter deposition rate is one monolayer per second, i.e.  $\sim 10^{15}$  atoms/cm<sup>2</sup> second or 200 Å/minute for a 'typical' atom of about 3 Å diameter. A contaminant gas having a partial pressure of  $10^{-6}$  torr will contribute a numerically equal flux at the substrate. Such contamination will be particularly effective if it is chemically active. The example in Figure 6-17 is from deposition by evaporation, at a higher rate (1200 Å/min) than the sputtering example, but the point is the same; the aluminium film begins to oxidize at an oxygen pressure  $\sim 10^{-7}$  torr. We must remember that a contaminant partial pressure of  $10^{-6}$  torr in a total sputtering pressure of 20 mtorr amounts to a contamination level of only 50 ppm! We are unlikely to achieve such a low level, and the contaminant flux will increase proportionately with its partial pressure. If the contamination results from an internal source such as outgassing from a heated substrate, then its partial pressure (which results from an equilibrium between the rates of introduction and pumping) can be minimized by maximizing the pumping rate and hence gas flow rate. (See Chapter 1, "Conductance"). But this expedient is ineffective if the contamination is introduced with the gas, indicating a vital need for pure sputtering gas.

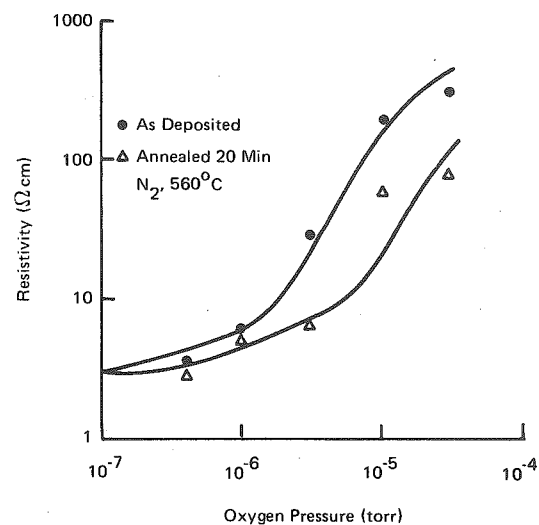


Figure 6-17. Room temperature resistivity vs oxygen pressure during evaporation of 5000 Å aluminium films at 200°C and 20 Å/sec (d'Heurle et al. 1968)



### Sputtering Gas Atoms — Fast and Slow

Compared with the fluxes of sputtered atoms and contaminants at the substrate, the flux of argon (or other sputtering gas) is truly enormous. At 20 millitorr, the argon flux would be about  $10^4$  times greater than the arrival rate of sputtered material. It would not be surprising, therefore, if argon were trapped in the growing film. Indeed, trapped argon is observed in sputtered films (Winter and Kay 1967), although not for the obvious reason. Winters and Kay evaporated a nickel film under similar conditions of argon pressure and deposition rate as for the sputtered films, but found that the argon content in the evaporated films was very much lower ( $< 1\%$ ).

They determined the content of their nickel films by vaporizing the film and measuring the resultant gas evolution with a mass spectrometer. The argon content was measured as a function of substrate temperature (Figure 6-18) and total argon pressure (Figure 6-19). The temperature dependence is as expected; argon is likely only to be physisorbed, so is less likely to be initially adsorbed and more likely to be subsequently desorbed, with increasing substrate temperature.

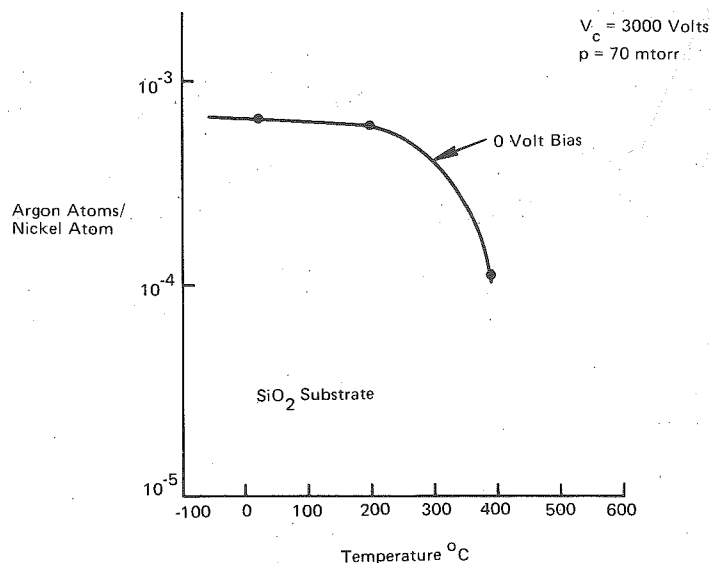


Figure 6-18. Argon content in sputtered nickel films as a function of deposition temperature (Winters and Kay 1967)

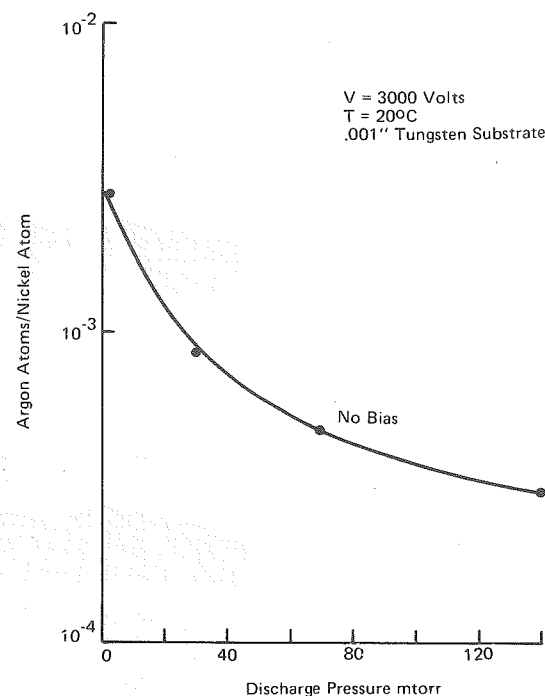


Figure 6-19. Argon content in sputtered nickel films as a function of argon discharge pressure (Winters and Kay 1967)

The pressure dependence (Figure 6-19) is rather interesting. The effect is ascribed to the small flux of high energy argon neutrals striking the substrate, rather than the large flux of thermal neutrals. Energetic argon ions striking the target are neutralized in the process and rebound as energetic neutrals. These energetic neutrals, arriving at the substrate, are likely to be embedded in the growing film; Comas and Wolicki (1970) have demonstrated how argon ions are entrapped in silicon, and fast neutrals are likely to behave in a similar way. Travelling across the sputtering chamber, the energy of these fast neutrals is attenuated by gas phase collisions and so their incorporation into the growing film (per unit film atom) decreases with increasing pressure.

One would expect fast neutrals to have a smaller collision cross-section than thermal neutrals. The existence of fast electrons and negative ions from the target similarly traversing the sputtering system without collision and bombarding

the substrate has been clearly demonstrated, as is discussed later. In the Winters and Kay work there is apparently an effect of the fast neutrals even at a pressure of 100 mtorr. Since there will be about one fast neutral leaving the target for each sputtered target atom, the measured argon content of  $\sim 10^{-4}$  argon atoms per nickel atom at 100 mtorr (Figure 6-19) implies that at least this proportion reach the substrate with enough energy left to be adsorbed. Based on collision probabilities (Chapter 1), this is a little surprising, but one can't argue with the results. It is presumably a manifestation of the lower collision cross-section and pronounced forward scattering that one expects for higher energy particles (see Appendix 4).

### *Excited Neutrals*

To return to Figure 6-16, we have so far been considering bombardment by ground state neutrals. A further source of bombardment is due to excited neutrals, of which metastables of the sputtering gas would be most abundant. These can presumably lose their potential energy at the growing film and hence influence its growth, although Kaminsky (1965) indicates that these metastables should be resonance ionized and Auger neutralized before they reach the substrate.

### *Positive Ions*

In addition to these neutrals, there will be bombardment by charged particles. Argon ions will be the most abundant positive ions, with a flux of the order of  $n\bar{c}/4$ . The figure of  $20 \mu\text{A}/\text{cm}^2$  from our example in Chapter 3 corresponds to a flux equivalent to a few tenths of a monolayer per second. There will also be ions of the sputtered material, produced both by electron impact ionization and by the Penning process of collision with metastables (Chapter 2, "Metastable Collisions"). These ions, and any others, will be accelerated across the sheath at the substrate. Under normal conditions, the sheath will be quite thin and there will be little attenuation of the ions due to collisions in the sheath.

Valuable information about ion bombardment at the substrate has been acquired via the work of John Coburn (1970 et seq.), who has been able to analyze the energy and mass of ions striking the substrate. His work is described in more detail in the section on bias sputtering. For now, we note that he was able to identify contaminant ions, the less abundant argon ion species such as  $\text{Ar}^{++}$  and  $\text{Ar}_2^+$ , and also complex ions such as  $\text{ArH}^+$  and short-lived ions such as  $\text{H}_3\text{O}^+$ . (We discussed in Chapter 2 how ions can change their chemical identity as their electronic shell structure changes). So we have to add these ions to our list in Figure 6-16.

### *Negative Ions*

Negative ions of the target material may form also. The space charge sheath established at the substrate will tend to repel and slow down these ions, but they will still reach the substrate if they are energetic enough (which will be so if they're formed at the target or in the target sheath). Negative ions at the substrate were detected by Koenig and Maissel (1970) in their work on sputtered quartz. Hanak and Pellicane (1976) have shown how fast negative ions from the target can sputter etch the substrate, and their findings have been confirmed more recently by the experimental work of Cuomo et al. (1978) and the theoretical work of Robinson (1979). Presumably, negative ions can also be formed from gas phase contaminants, although they would be energetic enough to reach the substrate only if they were formed in the target sheath.

### *Electrons*

A major source of charged particle bombardment at the substrate is due to electrons. With a conducting substrate, the average current density will be about  $1 \text{ mA}/\text{cm}^2$ , which is equivalent to  $6.25 \cdot 10^{15}$  electrons/ $\text{cm}^2$  second or a few electrons for each depositing atom. The majority of these electrons will be thermal electrons from the glow where they have energies of a few electron volts (Chapter 3), although only the more energetic of them will be able to surmount the sheath at the substrate. An insulating substrate on the anode in a dc discharge will charge up to floating potential and will receive a much smaller electron flux, equal to the ion flux.

In addition to these slow electrons, there will be bombardment by fast electrons. These electrons are emitted from the target by ion and other impact, are accelerated across the target sheath, and then travel across the sputtering system without making collisions, as described in Chapter 4. So they have energies equivalent to the sheath voltage. These electrons have been detected by Koenig and Maissel (1970); their results in an rf system, obtained by retarding potential measurements, are shown in Figure 6-20. Ball (1972), again using a retarding potential technique but in a dc system, obtained the results shown in Figure 6-21; these results suggest that a large fraction of the electrons striking the substrate have almost the full target sheath voltage, but it is not clear that an allowance was made for the transmission of the analyzer.

The energy spectrum of electrons bombarding the anode has also been measured by Leopoldo Guimarães (Chapman et al. 1974) using the apparatus shown in Figure 6-22. Typical results for the collector current as a fraction of the total current, using a copper target, are shown in Figure 6-23. For reasons involving the resolution and mode of use of the analyzer, these curves do not show electron flux against energy but rather power input to the substrate due to charged

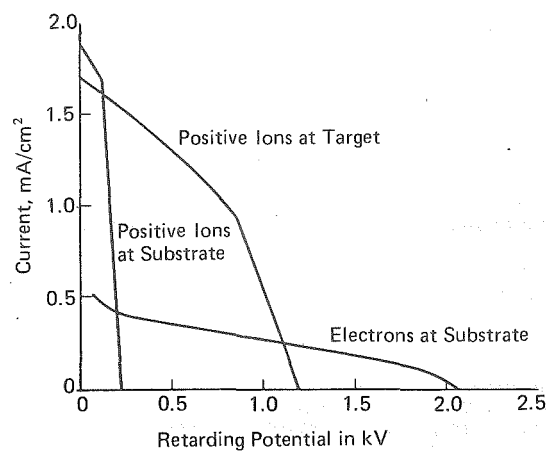


Figure 6-20. Electron and positive ion currents at substrate and target in an rf sputtering system (Koenig and Maissel 1970). Pressure  $\sim 5$  mtorr. Maximum ion energy  $\sim$  equivalent dc sheath energy.

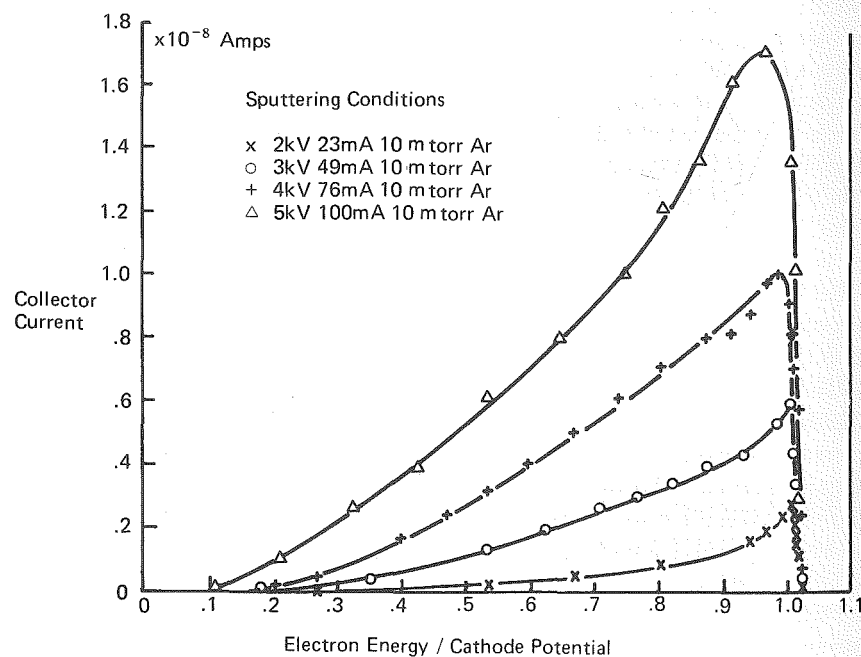


Figure 6-21. Energy spectra of secondary electrons arriving at the anode of a dc sputtering discharge (Ball 1972)

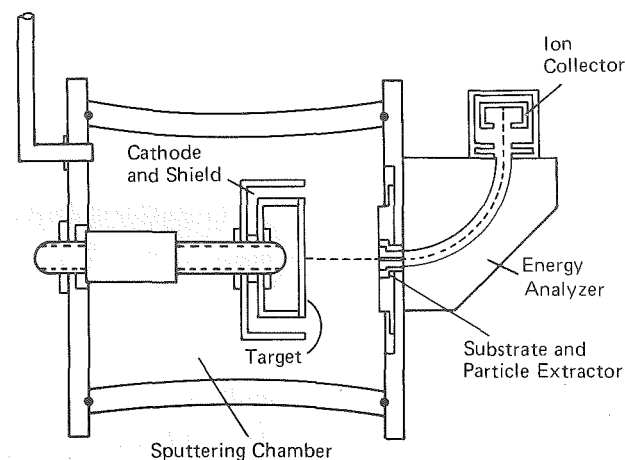


Figure 6-22. Energy analysis system for electrons on the substrate in dc sputtering (Chapman et al. 1974)

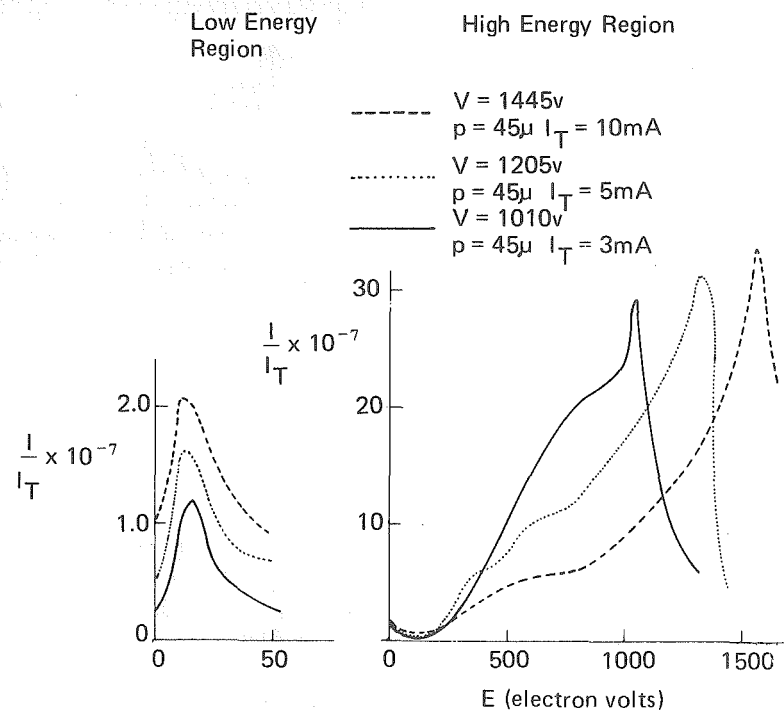


Figure 6-23. Energy spectrum for negative particles at the anode; note the different ordinate scales (Chapman et al. 1974)

particle bombardment versus particle energy, or, more precisely,  $dP(E)/dE$  vs.  $E$ , where  $dP(E)$  is the power carried to the electrode by particles with energies between  $E$  and  $E + dE$ . The flux distribution can be unravelled by noting that  $dP(E) = E dN(E)$ . The peak of the flux distribution occurs at quite low energy as expected, but there are a significant number of negative particles, which appear to be secondary electrons emitted from the target, that travel from the target to the substrate without making collisions, and hence travelling along the essentially straight field lines; we discussed these fast electrons in Chapter 4. This collision-free electron travel is presumably a manifestation of the total collision cross-section for electron scattering in argon (Figure 2-27) becoming quite small for electron energies above about 100 eV. However, although small in number, these electrons are responsible for almost all of the power input into the substrate. (The ion-electron recombination energy can also be considerable, amounting to  $4.5 \text{ mW/cm}^2$  for an ion current component of 0.3 mA).

In the same series of experiments, a composite sputtering target of copper and glass (Figure 6-24) was used in an rf sputtering system. The glass had a much larger secondary electron coefficient than the copper. The electron emission pattern was directly observed by coating a glass substrate with a fluorescent material and placing this on the counterelectrode of the sputtering system, several inches from the target. It was then possible to directly observe changes in the

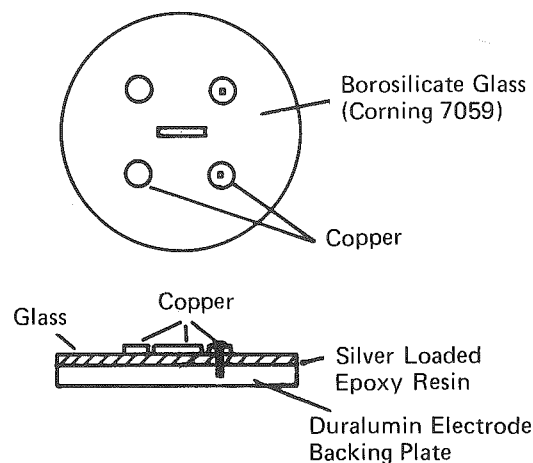


Figure 6-24. Composite sputtering target for secondary electron experiments (Chapman et al. 1974)

electron bombardment pattern as the sputtering conditions were varied. The threshold for glowing was at several hundred volts, so that only fast electrons were detected by the screen. The screen glowed very brightly opposite the glass sections of the copper/glass target. Figure 6-25a is a photograph of the fluorescent screen taken at an angle of about  $45^\circ$  through the vacuum chamber wall. The pattern on the screen could easily be deflected with a weak magnetic field (Figure 6-25b), showing the particles to be electrons rather than much heavier (and hence more difficult to deflect) ions.

These fast electrons can have a major influence on the structure and properties of the growing film on the substrate. The large energy input causes a good deal of substrate heating, and there are more subtle effects due to the electron interaction with the surface, as discussed in "Thin Film Formation". These electrons have been observed to discourage as well as enhance thin film growth (Chapman et al. 1974).

### Photons

The final type of bombardment that the substrate experiences is due to photons. Photons can be produced by ion or electron bombardment on any surface, and the photon can be as energetic as the ion or electron producing it, which therefore means a thousand electron volts or more in a sputtering system. Such energies put these photons in the soft x-ray class. Lower energy photons will also result from relaxation of excited atoms in the glow.

We have already discussed how photon bombardment can cause electron emission from a surface, and I would be surprised if these photons did not affect the growth of a film, as does every other type of energy input to the substrate. However, there appears to have been very little work on photon effects in thin film growth.

### Radiation Damage: Creation and Removal

There is a recent paper by DiMaria et al. (1979) on neutral charge traps produced in silicon dioxide films, actually in a reactive ion etching system which is nevertheless very much like a sputtering system. By measuring the centroid of the damage, they concluded that this damage was due to soft x-rays rather than charged particle bombardments. This conclusion is consistent with the additional observation that similar damage could be produced with the substrate anywhere in the system; photons, being uncharged, bombard all surfaces within the system. DiMaria et al. also found more gross damage at the surface of their samples, which they concluded was due to energetic ion, neutral, and electron bombardment. Their results are consistent with the earlier work by Hickmott (1969), who studied radiation damage in rf sputtered  $\text{SiO}_2$  films.

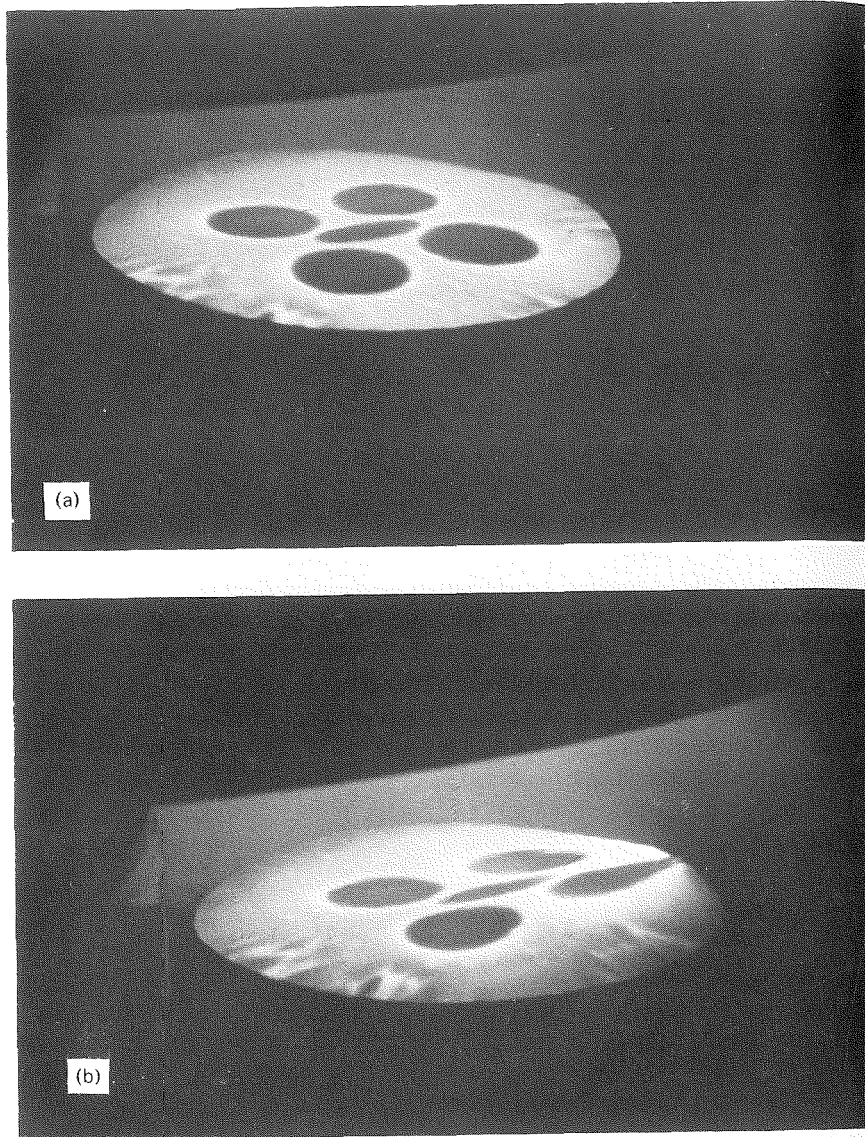


Figure 6-25. Fluorescence patterns on the counterelectrode screen  
 (a) without magnetic field  
 (b) with magnetic field  
 (Chapman et al. 1974)

There is a general observation that metallization of semiconductor devices in conventional sputtering systems leads to radiation damage of various types (neutral traps, interface states, etc.). The magnitude of the damage increases with increasing sputtering target voltage. Probably a similar photon bombardment mechanism is responsible for the damage. In order to minimize the damage, magnetron sputtering devices using lower target voltages are currently used for metallization; it seems to be necessary to reduce the target voltage below 500 V. We shall be discussing magnetron sputtering systems later in the chapter. Inconsistent with this sputtering experience, DiMaria et al. have not found any significant energy dependence of damage, at least over the range 300 V - 800 V in their  $\text{CF}_4$  reactive ion etching system.

The general phenomenon of radiation damage in thermally grown  $\text{SiO}_2$  due to the various microcircuit fabrication processes of sputtering, plasma etching, ion beam implantation, and e-beam lithography, has been reviewed by Gdula (1977). A more recent application of rf discharges is the *rf annealing* process, a method of removing radiation damage (Ma and Ma, 1977), or at least a way of removing charge states. The process consists essentially of exposing wafers to a low pressure rf discharge of fairly low power, inside a barrel type plasma etching system. The gas composition does not appear to be critical. The annealing mechanism is postulated to be a plasma assisted electrical-thermal effect.

### Bias Techniques

With so many particles bombarding the film, and with the sensitivity of the nucleation and growth processes to this bombardment, one would expect to be able to influence the properties of the film by changing the flux and energy of incident particles. It is difficult to directly modify the behaviour of the neutral particles, but the charged particles can be controlled by changing the local electric field, and this is the basis of the technique of *bias sputtering*.

### Voltage Distribution in Bias Systems

Figure 4-4 showed the distribution of voltage in a dc diode system when a voltage of -2000 V was applied to the target. The plasma potential  $V_p$  was at +10 V in that example. Suppose that we now electrically isolate the substrate platform from ground and apply a negative potential of 50 V to it (Figure 6-26). Electrical ground at 0 V is still present as the conducting parts of the chamber walls and baseplate. The plasma potential likes to remain positive with respect to everything in the chamber and, to a first approximation, will be unaffected by the negatively biased electrode, so that  $V_p$  remains at +10 V (Figure 6-27).

If the applied bias is  $V_B$  volts, then a sheath of potential difference  $V_p - V_B$ , which would be 60 V in the example, will be established in front of the substrate

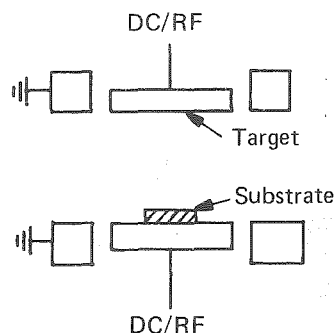


Figure 6-26. Schematic of a bias sputtering system

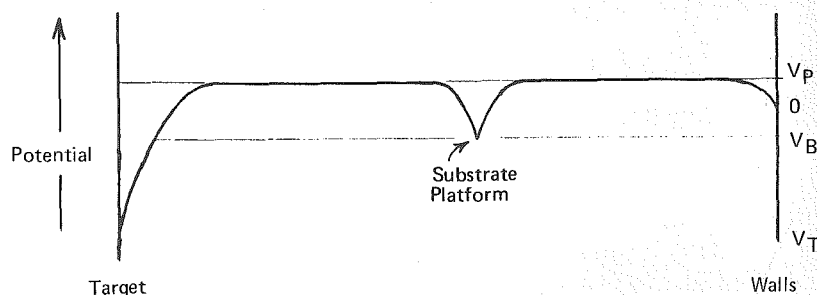


Figure 6-27. Potential distribution in a bias sputtering system

with polarity such as to accelerate positive ions onto the substrate. In effect, the substrate platform has become a secondary sputtering target. By this means, the flux and energy of all charged particles bombarding the substrate (Figure 6-16) can be modified. The energy of the ions striking the substrate would be equal to the energy with which they enter the sheath (which is usually small) plus the energy difference across the sheath, provided that there were no inelastic collisions en route. For small bias voltages, the sheath at the substrate will be thin enough that it will be collision free. For increasing bias voltage, the sheath thickness grows so that collisions may become important and attenuate the ion energy (Chapter 4, "Charge Exchange in the Sheath"). This means that the average energy of particles striking the substrate will increase less rapidly than the applied bias voltage. So a change in film properties as a result of bias sputtering may demonstrate the effects of a much smaller range of ion energies than is apparent.

If we tried to apply a positive bias potential, then we would encounter the results already discussed in Chapter 4: the plasma potential would rise so as to try to maintain the sheath in front of the bias platform, and the functions of the original anode and the bias table would interchange. This has been observed experimentally by Orla Christensen (1975) in a paper concerned specifically with voltage distributions in bias sputtering. He points out that a positive bias can cause sputtering of the (original) anode and consequent contamination.

Coburn and Kay (1972) have measured positive bias potentials slightly ( $< 15$  V) greater than the plasma potential, which implies that the sheath polarity has reversed. Although this result is not surprising for the very small probes that were used, and which would be limited by their small current-collecting surface areas, much the same result was found for very large positively biased probes. This unexplained result may have been due to the limited fast electron flux on the large probes due to their geometric shapes.

#### Bias — dc or rf?

An insulating substrate placed in a dc discharge will charge up to floating potential, and placing that substrate on a dc biased platform will not substantially change the situation until the substrate is coated with a conducting film, at which time the bias becomes effective. This situation can be changed by using rf bias, with the same rationale as for the sputtering of insulating targets. There is the same latitude in using dc or rf to power the main target, so that insulating films can be bias sputtered from insulating targets. The sputtering systems used become double ended. Figure 6-28 shows a system used for dc sputtering with rf bias. Systems with rf on both electrodes are probably more common.

It is usual, in both rf and dc bias sputtering systems, to measure the dc bias level with respect to ground. Although a more relevant parameter would be the sheath voltage — the plasma potential minus the bias potential — this is not easy to measure directly because of the relative inaccessibility (on a routine basis) of the plasma potential. The bias voltage is however a useful parameter to ensure reproducibility of the system.

It is probably true to say that, without the additional flexibility of bias sputtering, sputter deposition would be used to a much lesser extent than it is; the bias sputtering technique enables one to control so many film properties.

#### Control of Film Properties

Figure 6-29 shows how the resistivity of sputtered gold films can be controlled with the use of bias, reaching the bulk resistivity value for a bias of about  $-40$  volts (this figure refers to the dc offset of the rf waveform — see Chapter 5).



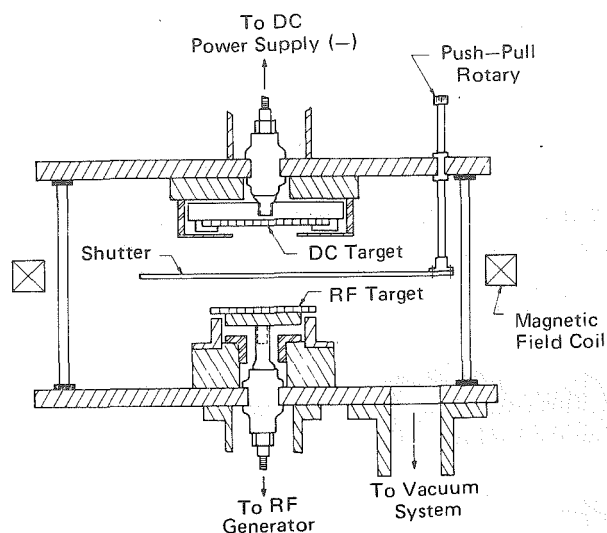


Figure 6-28. DC sputtering system with rf substrate bias (Vossen and O'Neill 1970)

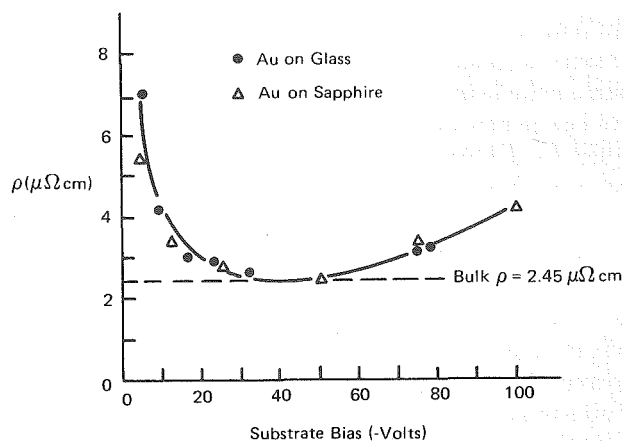


Figure 6-29. The variation of resistivity of 6000Å dc sputtered gold films versus rf substrate bias (Vossen and O'Neill 1968)

Similar behaviour of the resistivity change with bias for tantalum films is shown in Figure 6-30; this figure also illustrates the different effects of dc and rf bias discussed earlier in this section, with only the rf bias managing to achieve bulk resistivity.

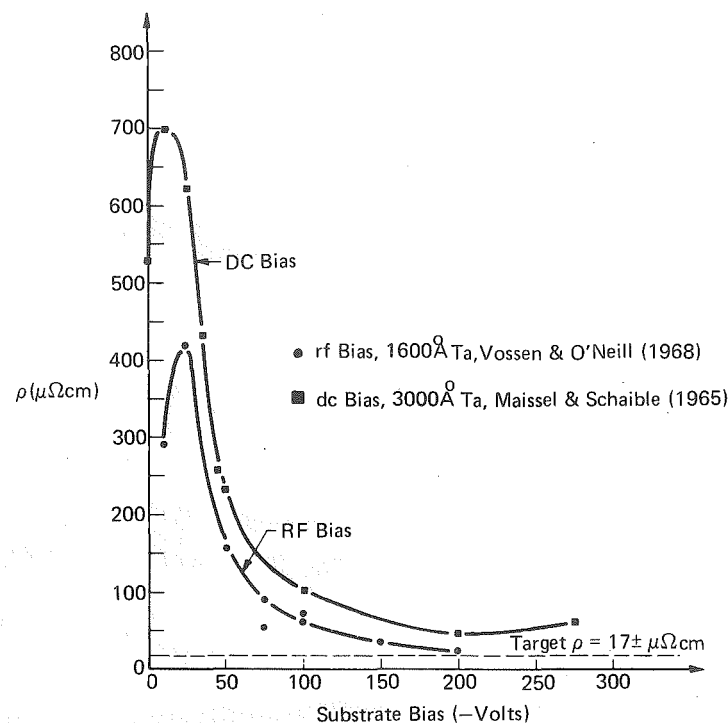


Figure 6-30. Resistivity of Ta films versus substrate bias for both dc- and rf-induced bias

- rf bias, 1600Å Ta, Vossen and O'Neill (1968)
- dc bias, 3000Å Ta, Maissel and Schaible (1965)

But bias sputtering is not restricted to control of electrical resistivity. It seems as though any and every thin film property can be controlled with this technique. Figures 6-31 to 6-33 show how the electrical properties of sputtered  $\text{SiO}_2$  films, the hardness of sputtered chromium films, and the etch resistance of sputtered silicon nitride films in buffered HF, can all be controlled by bias techniques — and there are countless other examples.

#### Control of Gas Incorporation

Earlier we saw that the sputtering gas can become incorporated into the growing film. The gas content also is a function of bias, and probably contributes to many other bias effects. Pursuing the work reported earlier, Winters and Kay (1967) measured the argon content of nickel films as a function of bias, and



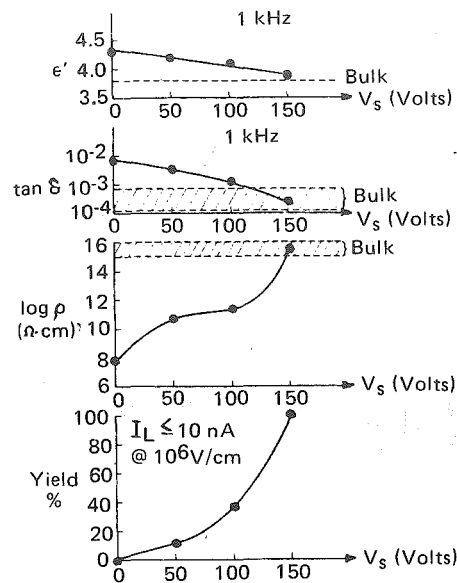


Figure 6-31. The dielectric properties of  $\text{SiO}_2$  films rf sputtered with rf-induced substrate bias (Vossen 1971):

- relative dielectric constant
- dissipation factor
- resistivity
- capacitor yield based on the criterion shown for capacitor areas of  $0.02 \text{ cm}^2$

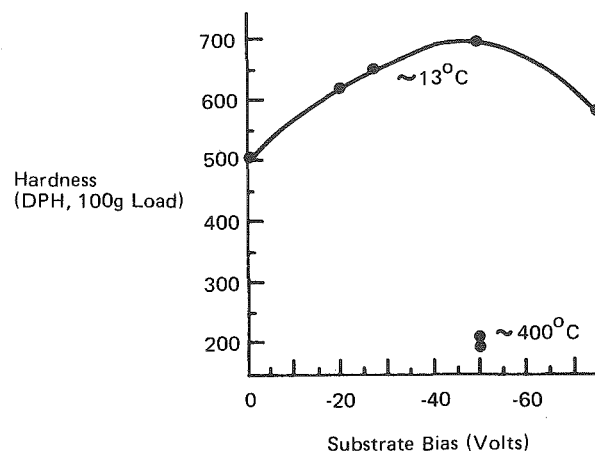


Figure 6-32. Influence of substrate bias voltage and temperature on hardness of sputter-deposited chromium (Patten and McClanahan 1972)

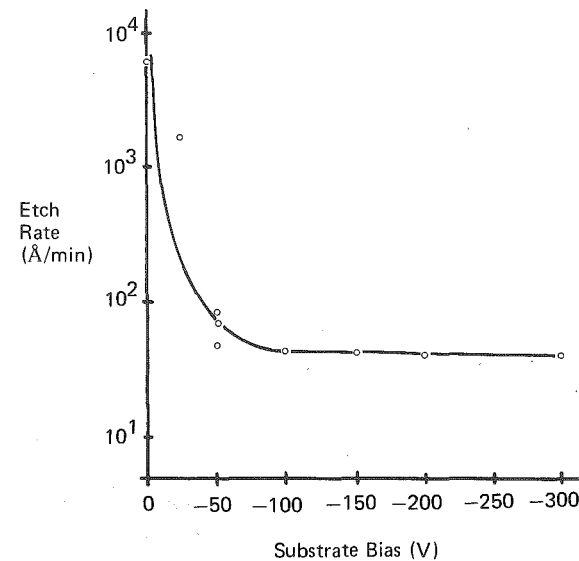


Figure 6-33. The etch rate of reactively sputtered silicon nitride films in buffered HF (Stephens et al. 1976)

their results are shown in Figure 6-34, with the 0-200 eV range clarified in the inset. The decrease in argon content observed is because incoming argon ions at these energies have a high probability of sputtering previously sorbed argon but only a small probability of sticking. However, as the bias voltage is increased, so is the energy of the incoming ions, and they are eventually energetic enough (at  $\sim 100 \text{ eV}$ ) to become embedded in the growing film; as soon as this effect dominates the sputtering effect, the argon content starts to rise again.

The growing film is also subject to resputtering by the incoming ions. However, you will recall from the discussion on sputtering target kinetics that the sputtering yield  $S$  drops rapidly below  $100 \text{ eV}$ , so at modest bias voltages of  $50 \text{ V}$  or so, there will generally be little resputtering of the growing film itself; but with more than  $100 \text{ V}$  bias, resputtering can be significant. We shall return to this point in "Deposition of Multicomponent Materials".

#### Application of rf Bias

Probably the most common configuration for bias sputtering is with rf on the target and rf bias. This can be accomplished in various ways. A single power supply is normally used, and the rf power is split between the target and sub-

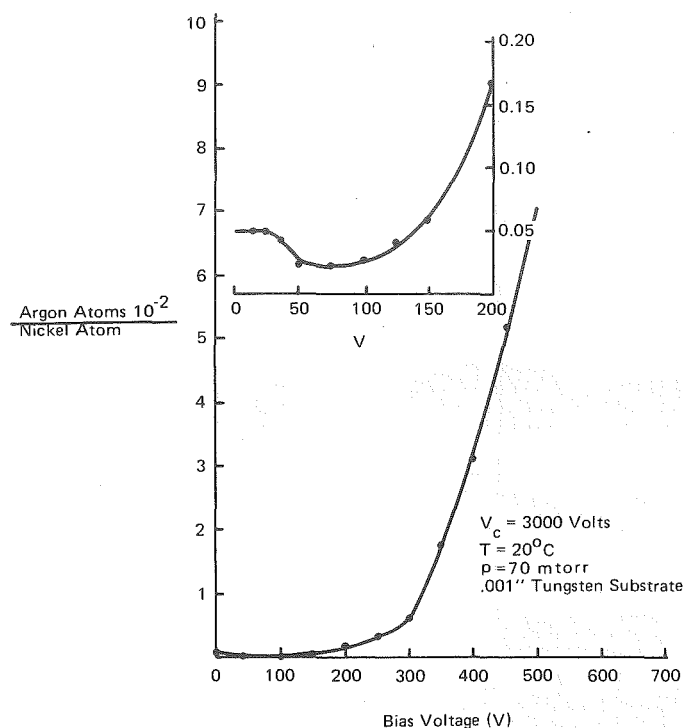


Figure 6-34. Argon concentration of sputtered nickel films, vs bias voltage (Winters and Kay 1967)

strate electrodes either in the matching network (for example with an autotransformer), or less frequently by inductive coupling (the *tuned substrate* system shown in Figure 6-35 and discussed in Chapter 5, "Equivalent Circuits of RF Discharges"), by capacitive coupling (Figure 6-36), or by using a controlled area ratio of electrodes — the *CARE* system discussed in Chapter 5, "Voltage Distribution in RF Systems". By contrast, systems with power more obviously applied to the bias platform are sometimes known as *driven substrate* systems. Keller and Pennebaker (1979) have analyzed the electrical properties of these various systems.

An alternative approach to the driven substrate system with one power supply is to use an rf power amplifier for each electrode with either a single common exciter or individual exciters. In the last case, exciters of nominally the same frequency (usually 13.56 MHz) are used, but they will never in practice be

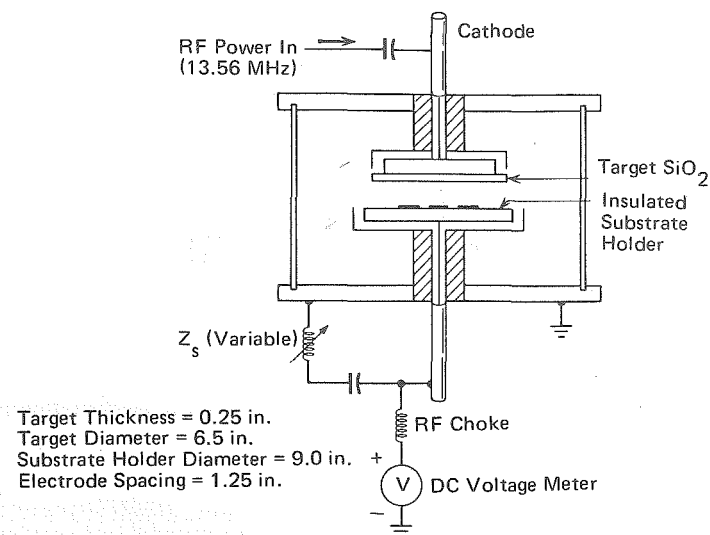


Figure 6-35. Experimental system for rf sputtering with substrate tuning (Logan 1970)

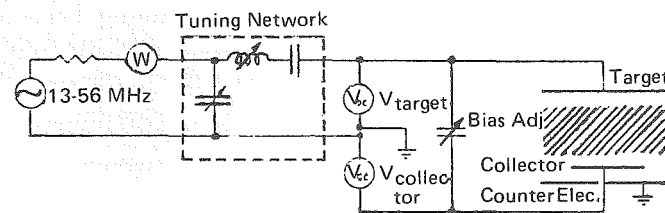


Figure 6-36. Circuit of RF sputtering diode with capacitive collector-to-target coupling (Christensen and Jensen 1972)

exactly the same, so that the phase angle between the two electrodes will continuously and regularly change. In all other cases, there will be a certain phase relationship between the two electrode sheaths that will be a function of operating conditions, cable lengths, and matching network settings. The effects of the phase relationship have been explored by Logan et al. (1977). The significance of substrate bombardment by fast secondary electrons from the target has been noted in the previous section. In rf sputtering with rf bias, these electrons will generally be decelerated by the substrate sheath to an extent determined by the phase of the sheath voltage as they enter. Logan et al. calculated and measured the maximum electron energy (Figure 6-37) and showed also how the threshold

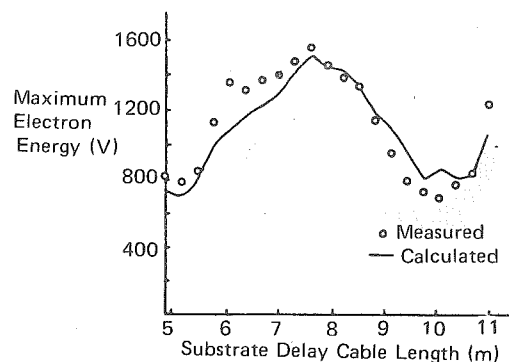


Figure 6-37. Maximum electron energy vs cable length, i.e. phase shift (Logan et al. 1977)

voltage of field effect transistor devices coated with sputtered quartz would be shifted during sputtering (Figure 6-38). The threshold shift increased with the maximum electron energy, and so could be phase controlled (which was achieved by varying cable lengths). As the maximum electron energy increased, higher annealing temperatures were required to anneal out the damage. Other parameters also might change with the phase angle.

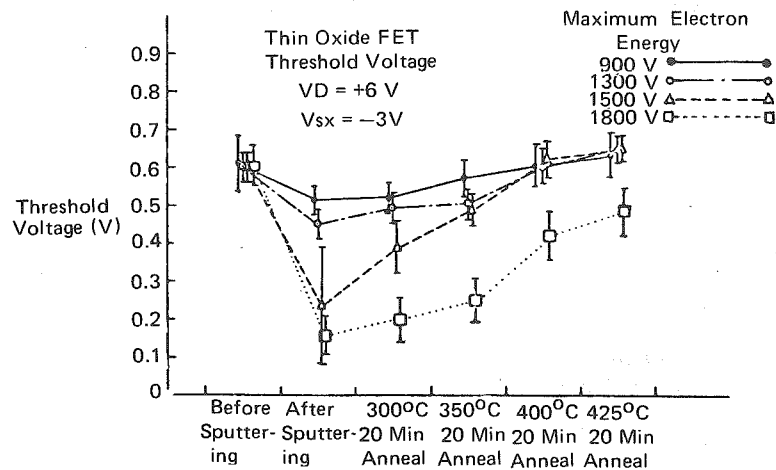


Figure 6-38. FET threshold voltage shift vs electron energy (Logan et al. 1977)

### Bias Sputtering Mechanisms

In a previous section, we saw that sorbed argon can be resputtered from the growing film by the bias sputtering technique. It is very common to find explanations for bias sputtering that describe how "... loosely-bonded material can be resputtered from the growing film by low energy ions". This may be an adequate explanation for the resputtering of weakly physisorbed gases, but it does not account for other commonly observed phenomena. As an example, sputtered chromium has a very high affinity for oxygen and tends to oxidize easily in the small amount of oxygen always present in a system; the use of bias sputtering can minimize this oxidation, even though the chromium-oxygen bond is very strong.

Winters and Kay (1972), in an extension of their earlier work on argon incorporation in thin films, studied the composition of films deposited in a gas mixture of argon and nitrogen. As a result of this study, they divided metals into three classes:

- metals which chemisorb molecular nitrogen and form a nitride, e.g. W.
- metals which do not chemisorb molecular nitrogen but still form a nitride, e.g. Ni.
- metals which neither chemisorb nitrogen nor form a nitride, e.g. Au.

Winters and Kay found that bias sputtering caused the nitrogen content of gold to increase, due to the increased sorption of nitrogen when the film was bombarded by energetic  $N_2^+$  ions. However, although this same effect is present with the tungsten and nickel films, it is overshadowed by resputtering of the previously sorbed nitrogen, as it was for the tantalum films in pure argon at low bombardment energies. This rather surprising result is a consequence of the sputtering yield for nitrogen on tungsten being rather large. Winters and Kay maintain that there is adequate evidence to conclude that most chemisorbed gases have large sputtering yields and low thresholds; they suggest that this is a consequence of the poor mass fit in the energy transfer function  $4m_1 m_2 / (m_1 + m_2)^2$  so that a struck chemisorbed atom cannot transfer its energy to the underlying substrate lattice. However, as we shall be discussing later in this chapter, there are examples in which a very thin metal surface layer, again having a poor mass fit to the substrate, has an anomalously low sputtering yield.

So it appears that bias sputtering can lead to either an increase or decrease in the concentration of gaseous species, depending on their surface adsorption characteristics which in turn control their sputtering yields. Winters and Kay also conclude that bias sputtering is unlikely to reduce impurity concentrations by more than a factor of 10, so that the biasing technique is not much of a substitute for good vacuum. However, Figure 6-39 shows how the nitrogen content

of metal films (unbiased) changes with the partial pressure of the nitrogen in the argon. Note that the nitrogen content of tungsten, which chemisorbs molecular nitrogen, decreases by less than a factor of 10 over four orders of nitrogen pressure change. So it may well be that, for tungsten and other class (a) metals, that biasing is very effective compared with decreasing the partial pressure of the contaminant.

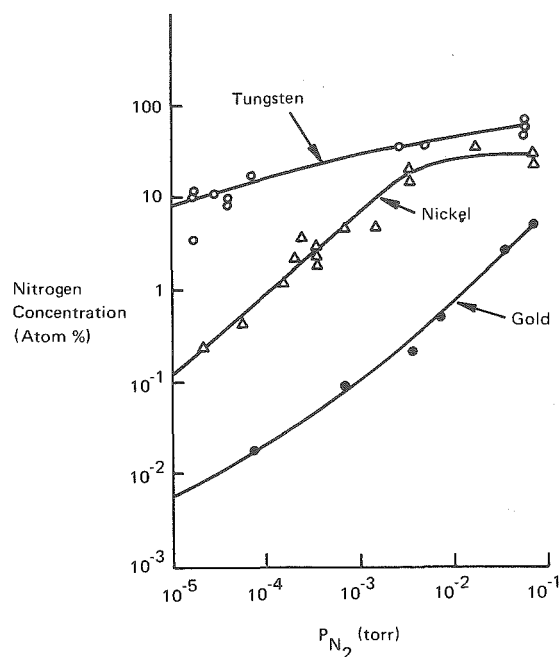


Figure 6-39. Nitrogen concentration in film vs partial pressure of nitrogen;  $p_{\text{tot}} = 70$  mtorr,  $T = 300$  K, target voltage = 3000 V, bias voltage = 0, and target - substrate distance = 4.5 cm (Winters and Kay 1972)

Winters and Kay make two other points. Firstly, they consider the effect of backscattering in the gas phase which tends to return sputtered material back to its substrate; they conclude that in many instances bias sputtering may be more effective in obtaining high purity films if the sputtering pressure is relatively high. Secondly, they note also that ion bombardment, and hence bias sputtering, also changes the physical appearance of a film. They had previously shown that

nickel films became much smoother as the bias voltage was increased from 0 V to 300 V. The topography of the film surface is important in determining its optical appearance, as light is scattered from surface features; we shall discuss more extreme examples of this later in the chapter. In Winters' and Kay's experiments, unbiased films of tungsten, nickel and iron looked dark grey or almost black, whilst biased films appeared metallic.

This last result emphasizes another point. Much of our discussion about bias sputtering so far has been concerned with the effect of bias on gas content. However, gas content is just one of many parameters which contribute towards the nature of a thin film. For example, the gold resistivity change in Figure 6-29 was apparently related to film density and not gas incorporation, and the tantalum resistivity modification in Figure 6-30 was due to a phase change. And other parameters such as the surface roughness or the hardness of a film may be important for a particular application.

Ion bombardment has many effects, some of which we are only now beginning to learn about; for example, in Chapter 7 we shall see how chemical reactions can be accelerated by ion bombardment. Changing the bias voltage will also change the power input to the film. The power due to ion bombardment can be considerable, and the consequent heating may be helpful or, as we shall see shortly, may lead to *grain growth* and other undesirable film features. We have also seen in earlier sections how fast electrons from the target can bombard the substrate. Increasing the bias on the substrate will tend to retard the electrons and lower their bombardment energy. Whilst this is always true in dc systems, the statement has to be restricted in rf systems depending on the phase of the sheath field seen by the fast electrons as they enter the substrate sheath. We discussed phase control in the previous section, and showed how it could be used to influence the threshold shift of FET devices during sputtered quartz deposition.

We would probably be correct to conclude that the control of the gas content of films is a significant role for biasing; but there are likely to be many other effects due to the flux and energy of ion and electron bombardment on the substrate. Some of these might be simple, such as thermal effects, and some might be more subtle influences on the nucleation and growth stages of the film. And in the next few sections we shall see how biasing can be used to control film topography by deliberately encouraging resputtering, but can also cause problems with multicomponent films by resputtering the film and causing a depletion of the component with the higher (or highest) yield.

There is no doubt that biasing can add enormously to the power of sputter deposition. As a broad generalization, it is likely that, no matter what particular film property you are interested in, it can be influenced by the bias sputtering technique. Try it and see!

### Analysis of Charged Particle Bombardment at the Substrate

In earlier chapters, the work of Davis and Vanderslice (1963) has been mentioned. They identified the mass and energy of ions bombarding the cathode of a dc discharge, as a means of understanding some of the target sheath phenomena. John Coburn (1970) has used the same approach, but applied to the substrate platform, with and without bias. This application has been extremely fruitful, covering quite a range of topics, and in our energy-conscious world, Coburn has to be congratulated on getting such good mileage out of the technique!

The experimental arrangement is shown in Figure 6-40. Some of the ions bombarding the substrate plane pass through a small aperture into a differentially pumped low pressure region, where they are first energy analyzed and then mass analyzed.

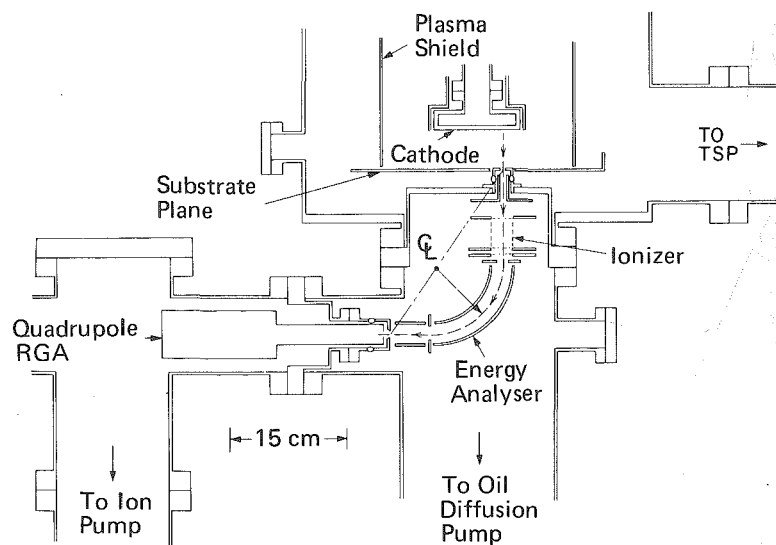


Figure 6-40. Experimental arrangement for the mass and energy analysis of ions bombarding the substrate plane (Coburn 1970)

This arrangement can be used to identify the ion species at the substrate as a function of their energy. Figure 6-41 shows 2 spectra of ions from a system sputtering copper. These spectra differ as a result of the energy analyzer being set to admit different energies. In this case the difference was 1 eV; the bias voltage was -30 V. The figure shows some of the complex and contaminant ions referred to earlier in the chapter.

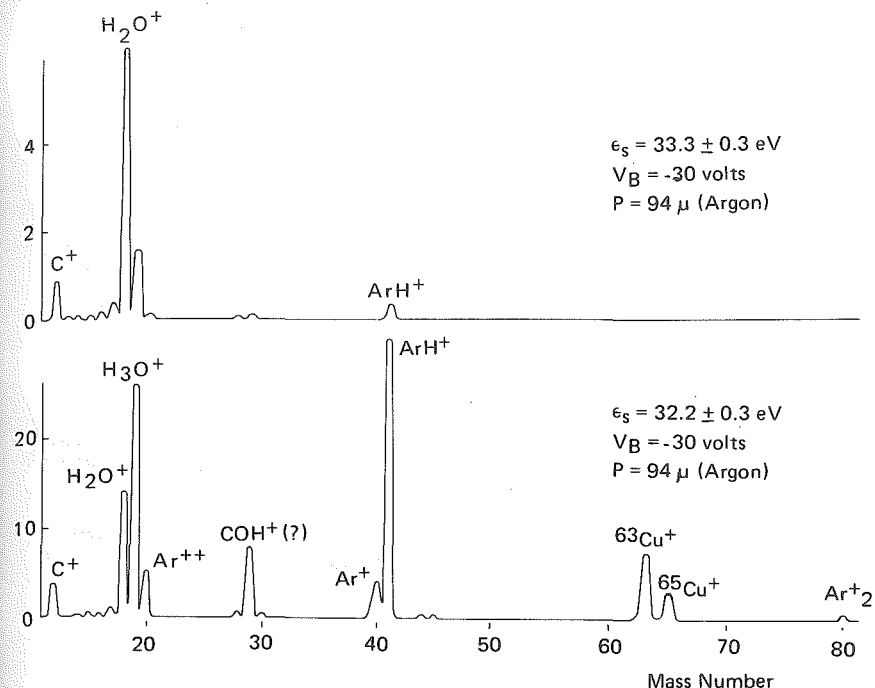


Figure 6-41. Mass spectra of positive ions from a dc discharge prior to sublimation pumping (Coburn 1970). Copper target -1000 V, cathode-bias table spacing 5 cm, argon pressure 94 mtorr, bias voltage -30 V.

Upper trace: analyzer set to  $33.3 \pm 0.3$  eV

Lower trace: analyzer set to  $32.2 \pm 0.3$  eV

The mass/energy analyzer can also be used to measure the substrate sheath voltage (plasma potential minus substrate potential) by looking at an ion such as  $\text{Ar}_2^+$ , which has a low cross-section for collisions in the sheath and a high mass so as to minimize energy modulation by the rf field as it crosses the sheath. The energy distribution will be strongly peaked at the sheath voltage. We have already discussed this application in Chapter 5.

Some of the sputtered target is likely to become ionized, particularly by the Penning mechanism of collision with a noble gas metastable, as discussed in Chapter 2. Copper has an ionization potential of 7.7 eV, well below the 11.6 eV metastable level of argon, and would be expected to be Penning ionized. Figure 6-41 clearly shows copper ions from the target.

The combination of an electron multiplier as an ion detector and a modern stable low-current amplifier, enables one to look at ion spectra with very high

gain. Figure 6-42 is a mass spectrum of ion bombardment on the substrate plane when a target half of copper and half of tantalum was sputtered in argon. In this case the energy analyzer was not used. If the ion fluxes from different mass numbers occur over a very wide range (in this case 6 orders of magnitude), the conventional approach is to take a series of spectra, with each subsequent spectrum having a gain increase of  $\times 10$ . Spectra for the Cu-Ta target example, taken by this means, are shown in Appendix 6, and are probably easier to interpret in that form. However, the series of spectra can also be taken in a single scan, with a useful savings in time, by using a logarithmic amplifier, as shown in Figure 6-42; actually this figure has a special non-linear logarithmic or *coburithmic scale*.

The largest ion currents in Figure 6-42 come from argon as expected. But the logarithmic amplifier reveals  $\text{Cu}^+$ ,  $\text{Ta}^+$ , and less abundant argon peaks at lower ion currents. For even smaller currents, less abundant isotopes and complexes appear, followed by contaminants such as  $\text{Nb}^+$  and  $\text{CH}_3^+$ . And so on. This expanded spectrum (and those in the appendix) show the sensitivity of the technique, and also illustrate one of the mixed blessings common to modern analytical techniques: the closer you look, the more you find.

Mass spectrometer data such as these have to be carefully interpreted, as the ion current magnitude cannot simply be equated with ion abundance; the quadrupole spectrum tends to underestimate higher mass ions, and its sensitivity also depends on ion energy.

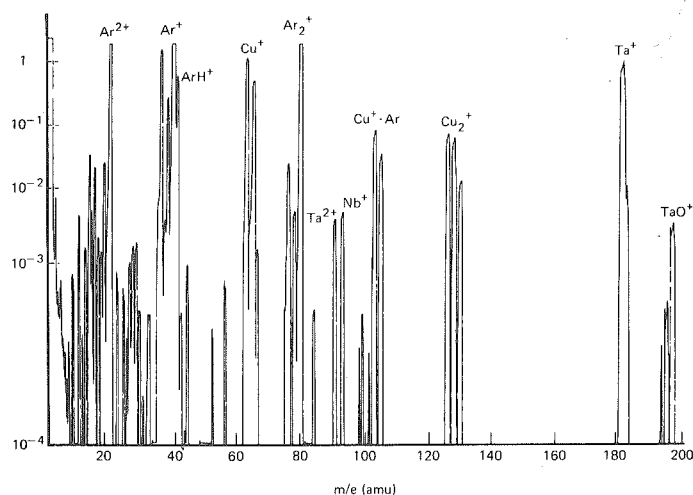


Figure 6-42. Ion mass spectrum at the substrate plane in an argon discharge sputtering copper and tantalum (Coburn 1979)

The mass/energy analyzer has been used by Coburn, by Coburn and Kay and other colleagues, for a variety of applications such as to measure the effects of discharge confinement on plasma potential, as described in Chapter 5, "Experimental Test of the Voltage Distribution Model". The sensitivity of the technique to the composition of a sputtering target makes it useful also as a technique for analyzing the composition in depth of the target as it is sputter etched away. The technique is then called *Glow Discharge Mass Spectrometry (GDMS)*, and is one of a series of techniques for *depth profiling* a sample, as discussed later in "Sputter Etching". In GDMS, one can employ noble gases with higher metastable states so as to encourage Penning ionization of the target components and so enhance the sensitivity of the technique.

I suspect that mass/energy analysis will continue to be useful in glow discharge analysis. Essentially the same technique has been recently used by Komiya et al. (1977) to study vapour deposition using a hollow cathode glow discharge.

### Bias Evaporation

So far we have been looking at the use of bias to control the properties of films deposited by sputtering. But the bias technique affects conditions at the substrate mostly, and in principle deposition could be by any technique, for example by evaporation. There are two manifestations of this combination, which are different in application rather than in concept. *Ion plating* is used primarily for high rate metal deposition with very large dc bias applied and is discussed further in the section on ion plating; *bias evaporation* is normally used with rf bias, with similar bias values as in bias sputtering.

Bias evaporation has been used by Vossen and O'Neill (1970) for the evaporation of aluminium. They suggest its use for any materials that recrystallize easily, and which would recrystallize under the energy input from a dc sputtering target. A schematic of the bias evaporation configuration is shown in Figure 6-43. Of course, to obtain any considerable amount of ion bombardment

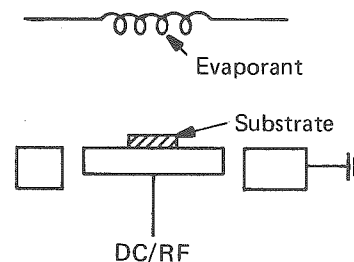


Figure 6-43. Schematic of a bias evaporation system

on the substrate, there must be a plentiful supply of ions, and these are obtained from a local glow discharge with substrate as target or part of the target. To obtain the discharge, the system is filled with argon to a pressure of a few millitorr.

Vossen and O'Neill reported several advantages of this technique over conventional evaporation. These advantages were in terms of being able to achieve almost bulk resistivity, ohmic contacts to silicon without sintering, reduced pin-hole density, conformal coverage over severe substrate topography (which is discussed further in the section on that subject), and smoother films. To elucidate the latter, aluminium films generally have a tendency to form 'hillocks' and to show microscopic pitting. With bias, these defects were less evident and reached a minimum at -400 V. For larger biases, the film started to show preferred {111} crystallographic orientation, and the surface roughened as grain growth became evident, probably due to the heating effect of the ion bombardment. However, we must note that some of the improvements were probably a result more of the sputter cleaning of the substrate just prior to deposition rather than of the ion bombardment during it.

#### Bias Sputtering For Conformal Coverage

Bias sputtering can be used to control *where* a film is deposited, so as to ensure conformal coverage of surface topography.

Coverage of "difficult" surface topography, of which a perpendicular step is the epitome, has long been a problem and is responsible for many device failures, such as an open circuit in aluminium metallization on a silicon chip (Schnable and Keen, 1971).

Conformal coverage is difficult because surface features act effectively as masks and/or present little surface area to the deposition source. Changing the type of deposition source usually alleviates one of these problems only by accentuating the other (Figure 6-44). Vossen (1971) has demonstrated that neither rotating the substrate table nor using planetary rotation offers a proper solution and that the same is true of straightforward sputtering; however, it must be added that some people *are* satisfied with the use of planetary rotation, at least to the extent that it eliminates failures, which is not the same as saying that conformal coverage was achieved.

Seeman (1966) showed how it was possible to uniformly coat the inside walls of deep narrow trenches by dc bias sputtering. Logan et al. (1970) have used re-sputtering to obtain better edge coverage with sputtered quartz films. Vossen (1971) has shown how biasing can similarly overcome the problem of metallizing steep walls. The basic principle used to cover the side walls is to resputter already deposited material and redeposit this on the side walls. This is facilitated by the sputter ejection pattern being under-cosine (Figure 6-45) for low energy bom-

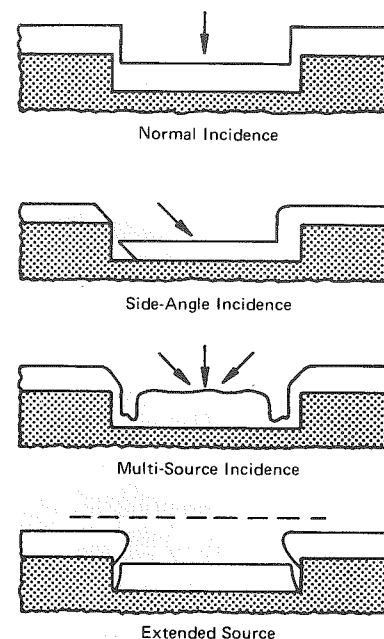


Figure 6-44. Defects arising as a function of source geometry during deposition of a coating to cover a steep step in a substrate (Kern et al. 1973)

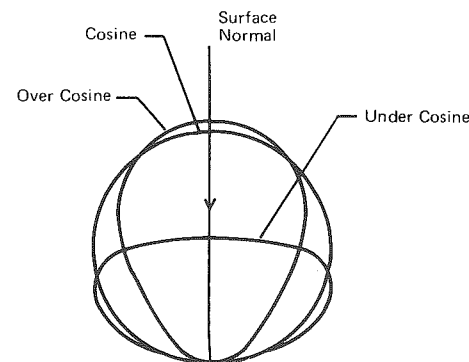


Figure 6-45. Angular distribution of particles from a polycrystalline target as a function of incident ion energy and direction (Kay 1962)



bardment; i.e. there is a tendency for material to be ejected sideways rather than outwards (cosine or over-cosine) as at higher energies. (The cosine law was initially derived from kinetic theory to describe the angular distribution of gas molecules bombarding a surface or leaving it. The result, which follows from an assumption of complete randomness of the motion of individual molecules, states that the number of molecules leaving the surface in a small element of solid angle  $d\omega$  at an angle  $\theta$  to the surface normal, is proportional to  $d\omega \cos\theta$ . The sputter ejection of atoms from a polycrystalline target is also a quasi-random process and tends to follow the same cosine law — to the extent already noted). As the bias voltage periodically varies, which it does (at mains frequency) for the usual rf or dc bias power supply to a greater or lesser extent (in this case, the greater extent is required — in other cases, we prefer to have a very small ripple), there is thus an effect which Vossen compares to a fireman hosing a wall up and down! There is little tendency for the material already on the side walls to be re-sputtered because the sputtering yield at virtually oblique incidence is practically zero (see later).

Vossen's experiments were performed using silicon substrates into which  $6\mu\text{m}$  high vertical steps had been anisotropically etched. Figure 6-46 shows the varying distributions of platinum dc sputtered onto the silicon test wafer at various rf-induced bias voltages. As the bias voltage is increased, relatively more metal is resputtered onto the side walls. Similarly, for a given bias voltage a greater proportion of material will be resputtered onto the side walls as the deposition rate is reduced. This is clearly a very useful technique for conformal coverage, but the parameters must be carefully chosen. In Figure 6-46, one sees again evidence of grain growth in the metal film. It is probably still true that people try to avoid having sharp corners rather than cope with them. Steep walls from etching processes can be turned into more gradual slopes by using 'taper control layers' (Kern et al. 1973) in wet chemical etching, or by using selective degradation of the photoresist in reactive ion etching, as described in Chapter 7, "Isotropic or 'Anisotropic' Etching?"

Finally in this section, we note the use of the bias technique to achieve not conformal coating, but almost its opposite — a deposited film with a planar surface, regardless of the topography of the substrate. This usage of bias sputtering for *planarization* (Ting et al. 1978) will be clearer after looking at the angular dependence of the sputtering yield, in "Sputter Etching".

#### Backscattering in Bias Sputtering

In an earlier section ("A Conventional DC Sputtering System — Choosing the Pressure Range"), we saw how molecules from a sputtering target can collide with gas phase molecules and be scattered, in some cases right back onto the target. This is a problem in bias sputtering, because the substrate backing plate

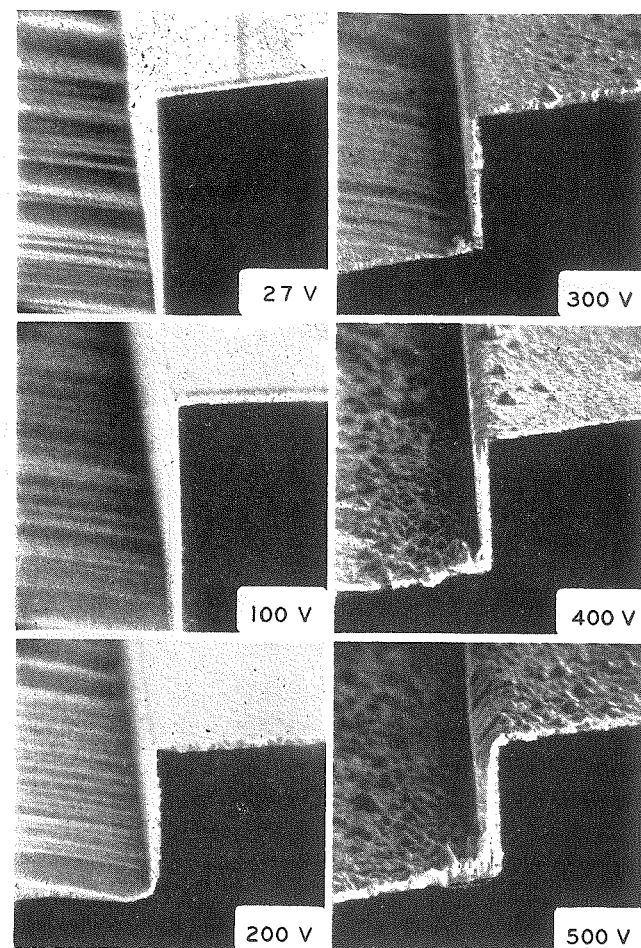


Figure 6-46. The thickness distribution of Pt coatings dc sputtered with various rf-induced bias voltages. The plane surface accumulation rate was held constant at 300 Å/min (Vossen 1971)

(Figure 6-26) will also be subjected to ion bombardment, and the resultant sputtering of the plate and backscattering in the gas phase can lead to backing plate material being deposited onto the substrate and incorporated into the growing film. A similar phenomenon of mixing would occur on composite targets, and would be important in sputter etching if not in sputter deposition. This problem has been investigated by Vossen et al. (1970). They placed 2.4 cm silicon wafers on various 15 cm diameter metal targets, principally Pt, in an rf diode sputtering system, with interelectrode separation of 5 cm. Using a dc level of  $\sim 700$  V on the rf target, they found that the platinum concentration on the silicon reached an equilibrium value after about 10 minutes. This equilibrium value ranged from about 1 monolayer at 2.5 millitorr to about 4 monolayers at 20 millitorr, showed little spatial dependence except near the edges of the wafer (Figure 6-47), and increased monotonically with pressure although showing signs of saturation. The equilibrium value is presumably a balance between deposition by backscattering, and resputtering. In this work the target voltages used were more representative of sputter etching than of bias sputtering, but note that although sputtering of the backing plate would be much slower at the lower voltages used in bias sputtering, so also would resputtering from the substrate. Vossen et al. did vary the target voltage over the range 500 V – 1200 V, and found that the platinum coverage on the substrate increased from 2 monolayers to 4.5 monolayers as the voltage was reduced to the lower limit. It would be unwise to extrapolate these results down to the 50 V or so frequently used in bias deposition, because the sputtering yields of materials change so rapidly with energy at such values.

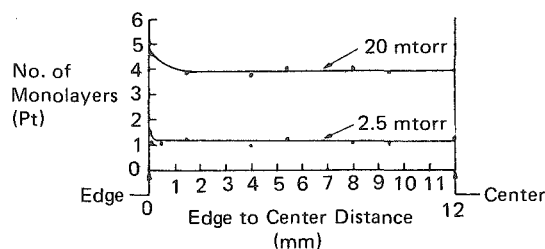


Figure 6-47. Typical wafer profiles; effect of argon pressure (Vossen et al. 1970)

The very clear lesson from these and similar results (Chang et al. 1973) is that one should use a backing plate which is at least compatible with the material being deposited, and may ideally be the same. The same message applies to the comparable situation in both types of diode plasma etching, as discussed in Chapter 7.

We shall return to the subject of backscattering in the section on "Sputter Etching", where we shall also see that there can be some very unfortunate choices of backing plate material.

### Deposition of Multicomponent Films

Most of our discussion to date has been concerned with the sputtering of single elements. But often multicomponent films are required, and these may be alloys, compounds, or a mixture of both. They can usually be prepared by sputtering from a single compound target, simultaneously from several different targets, by reactive sputtering, or by a combination of these techniques.

There are four stages that we have to consider, of the transport of an atom from a sputtering target to its incorporation into the thin film. These stages are sputter ejection from the target, transport through the gas, condensation onto the substrate, and stable incorporation into the film. We shall now consider these four stages.

### Alloys

Let's consider initially the deposition of an alloy film, and specifically we'll think about deposition from a Ni:Fe target of uniform 80:20 composition. When we first start to sputter the target, we'll be removing the layer of metal oxide that is inevitably on the surface of the target. During this period, the shutter must be interposed between the target and the substrate to prevent condensation onto the latter. After some while, which will probably be in the 5 minute-30 minute time range, the sputtering system will have stabilized and the surface oxide will be removed, revealing the metallic alloy. In dc sputtering, the removal of the oxide will be accompanied by a corresponding change (usually a decrease) in the discharge current, since the secondary electron coefficient of the metal and the oxide differ. Even if rf sputtering is eventually to be used, the use of dc sputtering to determine the time required to remove the surface oxide, is often extremely helpful, and this of course can be applied to single element sputtering as well as multicomponent.

Now the metal alloy surface, initially having an 80:20 composition, is exposed. But nickel has a slightly higher sputtering yield than iron; for 1000 eV argon ions, it's 2.1 for nickel and 1.4 for Fe (see Appendix 6). So if we used ions of this energy, the nickel and iron atoms would be sputter ejected from the target in the ratio  $80 \times 2.1 : 20 \times 1.4$ ; 86% of the atoms leaving the target would be nickel compared with 80% in the target. But this situation can't last for long, because a result of the preferential ejection of the nickel will be to cause the surface of the target to become enriched with iron. As this iron enrichment occurs, so the sputtering rate of iron atoms increases and of nickel atoms

decreases until they are again leaving in the ratio 80:20. Ultimately, in steady state, the departure rate from the target must equal the supply rate, which is the 80:20 alloy from the bulk of the target. In order to achieve this, in the present example, the surface composition would adjust to 72.7% Ni:27.3% Fe. During the period when the surface composition is stabilizing, the shutter must continue to be used to prevent condensation onto the substrate.

Two phenomena can prevent the steady state conditions described above, from being reached. The depletion of one element on the target surface (nickel in our example) will set up a concentration gradient of each of the elements at the surface, and this will encourage diffusion. In the case above, nickel will diffuse towards the surface and iron away from it; with enough diffusion, the initial 86:14 sputtering ratio could be maintained. Diffusion is minimized by keeping the target cold enough, and 'cold enough' will vary from alloy to alloy, of course.

Keeping the target cool will also offset another potential problem that can be encountered when sputtering multicomponent materials. If one of the elements or compounds has an appreciable vapour pressure at the target temperature reached, then it will evaporate from the target. Remember from Chapter 1, "Monolayer Formation Time", that a vapour pressure of  $10^{-6}$  torr would correspond to an evaporation rate of about 1 monolayer per second.

When the target has reached steady state, the shutter can be moved back and deposition can begin. Transport of the sputtered material from target to substrate will rarely be straight line travel. Even at the lowest sputtering pressures, collisions with the sputtering gas atoms will take place. As the pressure increases, transport becomes more like a diffusion process and some material is redeposited back onto the target. The redeposition does not affect the alloy composition because the target adjusts itself so that the *net* composition leaving the target is the same as the bulk. However, as the mfp of sputtered material decreases, more of it will eventually land on the walls and proportionately less on the substrate. There is no reason why the target atoms (Ni and Fe in the example) should have the same mfp, and so we should expect that the ratio of the Ni and Fe fluxes at the substrate will not be 80:20. On the other hand, the mfp values shouldn't be very different, so this will be only a small perturbation on the 80:20 value.

The next stage involves the condensation of the material onto the substrate. As we saw in the earlier section on "Thin Film Formation", an atom arriving at the substrate migrates around on the surface for a while, hopping from one adsorption site to another, until it either joins with another migrating atom to form a more stable pair, or it evaporates. The *condensation coefficient* is the proportion of the atoms arriving at the substrate that remains without evaporating, and this will be determined by the arrival rate, the bonding energy between adatoms and substrate, and the substrate temperature. In general, the condensation coeffi-

cient of each constituent of a multicomponent target will be different, causing an effective change in the composition of the depositing alloy.

Finally, the growing film will be bombarded by ions and so there will be a certain amount of resputtering of the growing film. As well as sputtering gaseous components from the film, the ion bombardment will sputter the solid components too. Since sputtering increases with increasing ion energy, such resputtering will be particularly effective under bias sputtering conditions. In the deposition of alloys, as at the target, the film will be depleted of the component with the higher sputtering yield. At the substrate, however, there will be no compensating mechanism.

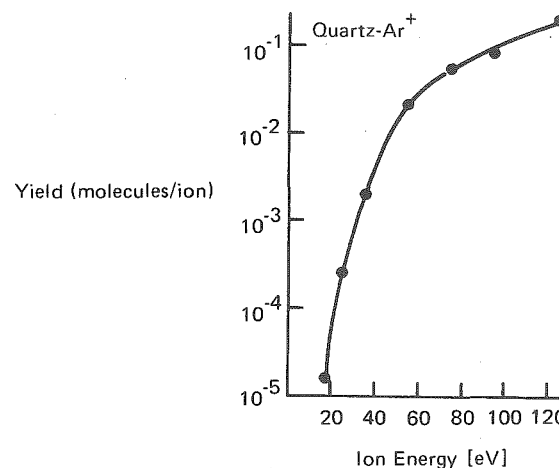


Figure 6-48. Sputtering yield of quartz in argon, in molecules per ion vs bombarding energy (Jorgensen and Wehner 1965)

Earlier in this chapter we have discussed sputtering primarily with rather energetic ( $\sim 500$  eV) ions. In bias sputtering, bias voltages of the order of 50 V are more common, and so low energy sputtering yield data becomes of interest. Figure 6-48 shows sputtering yield data for quartz in argon (Jorgensen and Wehner 1965). This data is typical also of the sputtering of metals, for which more yield data, obtained by Stuart and Wehner (1962) using an optical spectroscopic technique, is shown in Appendix 6. What is commonly observed is that the yield, which decreases linearly as the ion energy reduces from 1000 eV to 100 eV, starts to decrease much more rapidly somewhere below 100 eV; n.b. the logarithmic vertical axis in Figure 6-48. An apparent threshold is observed, although this is influenced by the sensitivity of the detection technique. Table 6-2 shows

Table 6-2 Threshold Energies (Stuart &amp; Wehner 1962)

	Ne	Ar	Kr	Xe	Hg
Be. ....	12	15	15	15	
Al. ....	13	13	15	18	18
Ti. ....	22	20	17	18	25
V. ....	21	23	25	28	25
Cr. ....	22	22	18	20	23
Fe. ....	22	20	25	23	25
Co. ....	20	25	22	22	
Ni. ....	23	21	25	20	
Cu. ....	17	17	16	15	20
Ge. ....	23	25	22	18	25
Zr. ....	23	22	18	25	30
Nb. ....	27	25	26	32	
Mo. ....	24	24	28	27	32
Rh. ....	25	24	25	25	
Pd. ....	20	20	20	15	20
Ag. ....	12	15	15	17	
Ta. ....	25	26	30	30	30
W. ....	35	33	30	30	30
Re. ....	35	35	25	30	35
Pt. ....	27	25	22	22	25
Au. ....	20	20	20	18	
Th. ....	20	24	25	25	
U. ....	20	23	25	22	27

the threshold data obtained by Stuart and Wehner, corresponding to a detection limit  $\sim 10^{-5}$  atoms/ion. They observed no correlation between thresholds and energy transfer functions, and concluded that a binary sputtering model is inappropriate at these energies, in accord with more recent theories.

In a later section on "Sputter Etching", I shall describe some work by Tarnag and Wehner (1972) that shows how the sputtering yield of some thin film materials varies enormously according to the thickness of the film and the nature of the underlying substrate. There is very likely to be a comparable effect in bias sputtering, compounded if one is depositing a multicomponent film. Under such

circumstances, sputtering yield data from homogeneous targets is probably of little relevance.

Taking all of these various effects together, we can see that the composition of a sputter deposited alloy film can be quite different from that of the target. However, the composition change should be reproducible for a given set of conditions, and so it becomes mainly a matter of choosing or fabricating a target of appropriate composition.

There are two other points to be noted. Firstly, a sputtering ratio of the two elements in the target holds for a particular ion bombardment energy. If that energy changes, e.g. by changing the target voltage or by changing the pressure, there will be a transition period while the target surface adjusts to a new steady state composition. Secondly, the composition of the deposited film can be changed somewhat by adjusting the bias voltage and other process parameters, but this means may be inconsistent with other process requirements. More flexibility may be attained by using two (or more) quasi-independent targets. One would then need to consider the deposition uniformity problems posed by the geometric constraints of this arrangement, as well as by the beam-like nature of electron and negative ion (if present) bombardment of the substrate. Nevertheless, this can be done successfully, with adequate confirmation from the deposition of multicomponent magnetic films.

### Compounds

We now turn to consider the sputtering of a chemical compound target. Is this target sputtered as molecular species or as atoms? The general answer is both. The question has been studied by Coburn et al. (1974), who also cite several other papers where sputtered molecular species were detected.

Coburn et al. studied the rf sputtering of metal oxides. Using the ion sampling and analysis system that was described earlier in the section on bias sputtering, they have looked specifically at the relative numbers of atomic metal ions and dimeric metal oxide molecular ions arriving at the substrate plane. In some cases, ternary and more complex molecular ions were observed but always at very low intensities. Coburn et al. presented their data in terms of  $\eta = \text{MO}^+ / (\text{M}^+ + \text{MO}^+)$  for a series of metals M. They found that  $\eta$  was strongly influenced by the relevant M-O bond strength, as shown in Figure 6-49. Not surprisingly, more strongly bonded metal oxide ions were less likely to be disassociated. Whilst  $\eta$  is defined and measured for ions, one would expect this ratio to be at least indicative of the corresponding neutral species, and probably numerically not so different. Coburn et al. also found that  $\eta$  decreased significantly with increasing pressure, and since  $\eta$  at zero pressure is likely to be the best representation of the ion ratio leaving the target (there being no collisions in this hypothetical

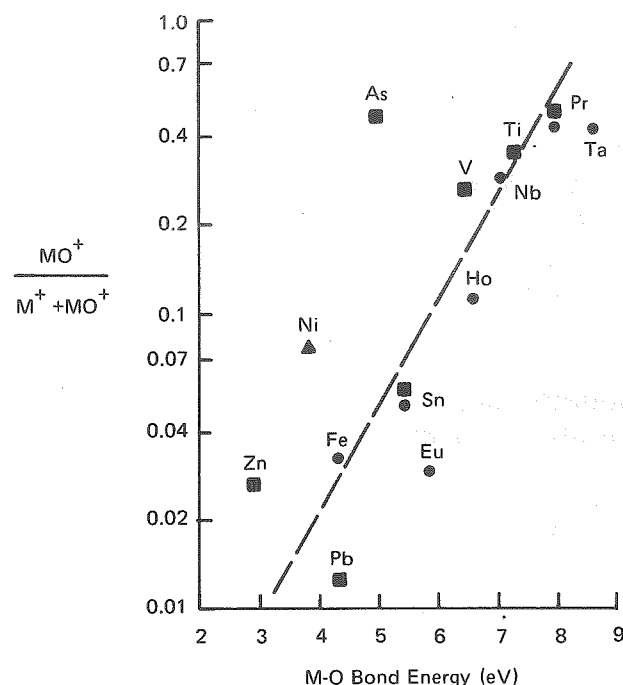


Figure 6-49. The dependence of  $MO^+/(M^+ + MO^+)$ , i.e. the relative ion flux of the dimer, on the bond energy M-O. Argon pressure 60 mtorr, rf power 100 watts at 13.56 Mhz, target area 20 cm<sup>2</sup> (Coburn et al. 1974)

case), the  $\eta$  values shown would tend to underestimate the relative concentration of the sputtered molecular ion.

Figure 6-49 and other results indicate that the M-O bond strength is not the only factor influencing  $\eta$ . Coburn et al. propose that a molecular sputtering event is more likely to occur if the atom struck by the bombarding ion can transfer enough energy to its molecular partner that they can be ejected as a pair. The energy transfer function (Chapter 1, "Energy Transfer in Binary Collisions") tells us that this is more likely when the atom masses are similar, and in Figure 6-49 it is certainly the lighter metals, with smaller mass ratios compared to oxygen, that lie above the line and exhibit larger molecular ion fluxes than a direct dependence on the M-O bond would suggest. Finally, Coburn et al. demonstrate that the presence of contaminants such as water vapour, has a marked effect on the ratio  $\eta$ .

### Restoration of Stoichiometry

Given that a metal oxide target, and by implication any other compound target, is unlikely to be completely sputtered in a molecular form, it is not surprising that the stoichiometry of the resulting thin film will be different from that of the target, usually being deficient in the gaseous or other volatile species. For example, films from a quartz target sputtered in argon tend to be deficient in oxygen. This can be compensated for by sputtering in a mixture of 95% Ar:5% O<sub>2</sub> (Erskine and Cserhati 1978). The oxygen served to fully oxidize the sputtered film and so restore its stoichiometry. It can be particularly effective in doing this because the glow discharge environment provides energetic electrons to dissociate the molecular oxygen into its chemically more active atomic form.

We should note that we do not always want to achieve the stoichiometry of the equivalent bulk material. For example, Mogab et al. (1975) found that silicon nitride films which met their requirements were richer in nitrogen than the stoichiometric Si<sub>3</sub>N<sub>4</sub>.

### Reactive Sputtering – Again

But if we are going to react a small amount of Si or SiO with O atoms, why not a lot? Indeed this can be done, and sputtered quartz films can be fabricated by sputtering a very pure elemental silicon target in a 50% Ar:50% O<sub>2</sub> mixture (Erskine and Cserhati 1978). This is the process of *reactive sputtering*, the chemical combination of the sputtered species and a component in the gas phase, that we usually try to avoid. Reactive sputtering can be used to promote total chemical conversion of the target material or, as in the previous section only to compensate for a deficiency in the film.

Quite small quantities of gas can be very effective and quite critical, so that careful partial pressure control, e.g. by mass spectrometry, is required. Note though, that although partial pressures of reactive gases can be very low, one still needs an adequate supply or flow of reactive gas. This requirement is discussed in more detail in the next chapter on "Plasma Etching". Oxygen and nitrogen are frequently used in reactive sputtering. In the discharge, molecular ions will be formed, and diassociation will lead to atomic ions and atomic neutrals in ground and excited states. Each of these species can play its role in the chemical conversion of the film.

The general situation will be rather complex and it is more fruitful to pursue specific cases. In principle, reactions could take place on the target, in the gas phase, and on the substrate. Target reactions result in one actually sputtering a compound target. These usually have a lower yield than elements, and result in the often observed reduction in deposition rate with added reactive gas.

Gas phase reactions suffer from the same problem of conserving energy and mo-

mentum that was discussed in Chapter 2. However, since there is in this case a molecular product, there is a chance that surplus energy will be absorbed into vibrational and rotational transitions, so such reactions should be much more likely than in atomic ion-electron pair recombination. On the other hand, there seems to be a general opinion that more reaction under these circumstances takes place on the substrate.

We have already discussed some of the various bombardments that go on at the substrate. We now add bombardment by reactive positive ions and neutrals to the list. Relevant work by Winters and Kay on the effects of the sorption characteristics of various gaseous and ionic species has already been cited. In the case of electronegative gases such as oxygen, we shall also have bombardment by fast oxygen negative ions formed in the target sheath or on the target itself. Then add substrate bias to confuse things!

There are all sorts of peculiar and interesting effects in reactive sputtering; they usually turn out to be due to some of the effects we have noted. For more practical information, see the review articles by Holland (1956) and by Maissel (1970), and the extensive bibliography by Vossen and Cuomo (1978).

## SPUTTER ETCHING

*Sputter etching* is the name conventionally given to the process of removal of material from a surface by sputter ejection. There are several uses for the process other than as a prerequisite for sputter deposition, as we have already discussed.

### Pattern Production

If material is selectively removed from a surface by using a suitable mask, then an etch pattern can be produced. The process of sputtering is fairly universal, so that the variety of wet chemicals used for the same process can be eliminated. Since sputtering results from bombardment by ions that move along electric field lines, and because field lines are always perpendicular to an equipotential surface, then etch profiles are inherently vertical in contrast to the isotropic profiles observed with wet chemical etching (Figure 6-50).

Sputter etching can be carried out in a conventional sputtering system with an in situ glow discharge, or with an externally generated ion beam. Ion beam sources are themselves glow discharge devices and are discussed in a later section. The change with an ion beam system is that the operating pressure can be much lower ( $< 10^{-4}$  torr). There is then less chance of sputtered material (from the target or more importantly from the mask or target support) colliding in the gas phase and being backscattered onto the target. There is also a negligible flux onto

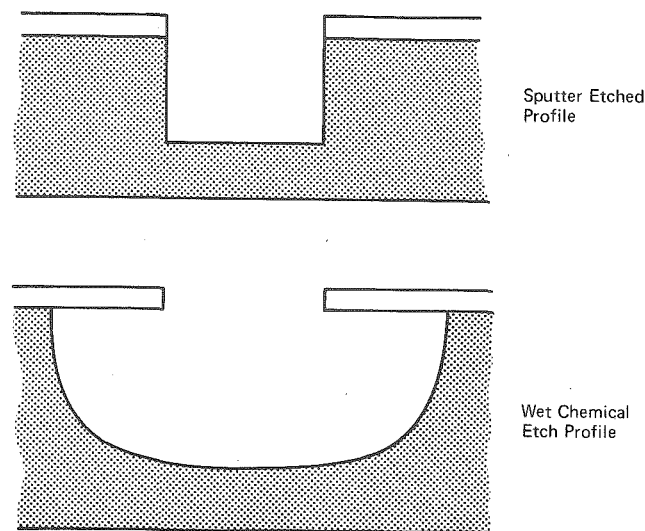


Figure 6-50. Etch profiles produced by sputter etching and by wet chemical etching.

the target of energetic neutrals produced by charge exchange. These fast neutrals are not affected by the electric field and therefore do not follow the field lines onto the target. They could lead to undercutting of the mask. In practice, there is a noticeable difference of directionality between results obtained in sputtering and ion beam systems. The difference is not that great, however; this may be due to pronounced forward scattering of the ions neutralized in the charge exchange process, so that the fast neutrals are more directional than one might at first suspect.

But even for ion beam systems, the sputter etch profile shown in Figure 6-50 is rather idealized. Two prime reasons for this are *mask erosion* and *trenching*. If the mask itself is also etched by the sputtering process, and this is always the case to some extent, then the final dimension of the opening in the mask will be greater than the initial dimension, leading to a tapered profile (Figure 6-51). The propensity of the mask to be sputter etched depends on its thickness and its profile. For etching of small dimensions of the order of microns, lithographically processed patterned photoresist materials are used. To achieve such resolution, the resists have thicknesses  $\sim 1 \mu\text{m}$ . The polymeric materials used for photoresists tend to sputter rather easily and also degrade under ion bombardment. Sometimes the heating effect of the glow causes *resist flow*, so that its profile changes. These effects combine to make resist masks prone to etch back during sputter etching.



There are much more resistant etch masks. Oxides generally have low sputtering yields, and alumina and magnesium oxide make good masks. But they are not photosensitive, so they must be patterned using more conventional photoresist

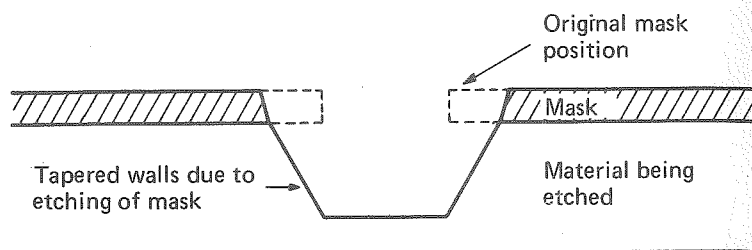


Figure 6-51. Etch profile resulting from mask erosion.

masks. The additional steps of oxide deposition and etching must be weighed against the reduced mask erosion.

*Trenching* is the enhanced erosion around the foot of an etched wall, leading to the 'molar' shape shown in Figure 6-52. It results from the increased flux of ions at the trenches due to reflection off the side walls of the etch pit, and perhaps also from material sputtered from the side wall onto the base of the pit.

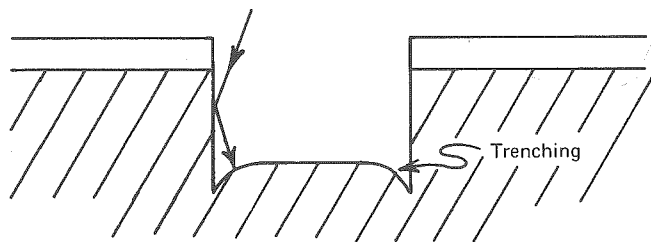


Figure 6-52. 'Trenching' in sputter etching

Several other phenomena control the topography of a sputter etched target. One concerns the redeposition of sputtered material. In the section on bias sputtering, we saw how some material is sputtered sideways, and this can be redeposited onto the side wall of another feature. This effect can be further illustrated by some results of Glöersen (1975). During the sputter etching of aluminium using a photoresist mask (actually in an ion beam system, but the principle is the same), sputtered aluminium is redeposited onto the side wall of the resist. After processing, the resist is chemically removed, leaving a wall of metal around the original resist position.

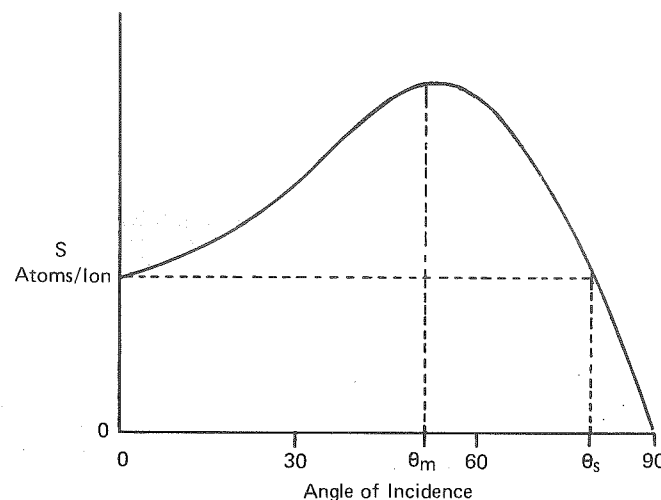


Figure 6-53. Variation of sputtering yield with angle of incidence (with respect to the target normal)

Another phenomenon related to etch topography depends on the angular dependence of sputtering yield. Figure 6-53 is a generalization of the effect; there are many specific examples, e.g. Wehner (1959), Cheney and Pitkin (1965), Glöersen (1975). Normal (in the angular sense) sputter ejection due to normal ion incidence requires  $180^\circ$  reversal of the momentum; this is not very likely and accounts for the low energy efficiency of the sputtering process. As the angle of incidence increases, so does the sputtering yield, again for momentum considerations. This is accompanied by the sputter ejection angular distribution becoming pronounced in the direction of specular reflection. Ultimately the yield goes to zero at  $90^\circ$  incidence, resulting in a maximum yield somewhere between  $0^\circ$  and  $90^\circ$  depending on the target material, and the ion identity and energy. This angular dependence has several consequences. One is the formation of *facets*. Figure 6-54 shows two surfaces being etched, one normal to the ion beam and the other at angle  $\theta$ . If we consider sections of each surface that present the same cross-sectional area  $A$  to the incoming beam, then we can see that the etch rates in the direction of the beam,  $R_b$  and  $R_c$  respectively, will be proportional to the sputtering yields at the relevant angles of incidence. Although the inclined surface is subjected to a lower flux of ions, this is irrelevant because the volume of material removed depends on the *cross-sectional* area and the etch rate.